A Prediction of the 21cm Angular Power Spectra in IDE Scenario for BINGO and SKA

Linfeng Xiao André Costta

Bin Wang

Outline

- Intensity Mapping
- Interacting Dark Energy (IDE) Model
- 21-cm Angular Power Spectrum
- Fisher Matrix Analysis
- Conclusions

Work Proposal

- We aim to see the *effects of IDE* on 21-cm angular power spectrum via varying interacting parameters λ_1, λ_2 and the equation of state w
- We have modified a new version of python CAMB with *IDE* scenarion considered and made it nested in a *self-developed* code for calculating 21-cm angular power spectrum
- For a qualitative discussion, we set a central redshift of $z = 0.28$ for BINGO
- The cosmological parameters of ΛCDM and the IDE model here are *best-fit* values from Planck 2018
- A *Fisher matrix* analysis is carried out in order to forecast the parameter constraints for BINGO and SKA in the context of IDE scenarios

Intensity Mapping

- IM is a technique aims to map a single emission line from multiple unresolved galaxies, each of which is below the detection limit, but resolves large-scale structures by measuring intensity fluctuations over cosmological distances. Chen et al. 2019

- The advantages of HI IM over optical galaxy surveys: Olivari et al. 2018

  a) a large volume of the Universe can be surveyed within a relatively short observing time;

  b) the redshift comes directly from the measurement of the redshifted 21-cm line;

  c) all the signal is recorded, including gas in between galaxies;

  d) HI is expected to be a good tracer of mass with minimal bias.

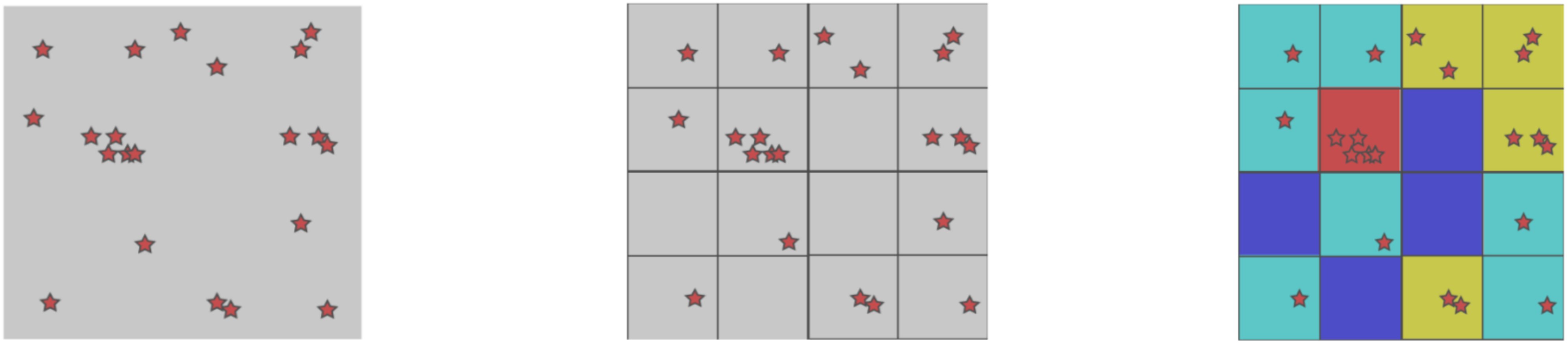

Interacting DE Model

- ΛCDM faces *challenges*:

  H_0 tension, σ_8 tension, Λ problem, coincidence problem ...

- *Go beyond* standard cosmology:

  Quintessence, modified gravity, decaying DM, interacting DE ...

- *Unclear nature* of DM and DE:

  any energy transfer?

  difficult to describe the interaction or dynamics from first principles, but easier from phenomenology.

Interacting DE Model

- The *Formalism*:

$$\dot{\rho}_c + 3\mathcal{H}\rho_c = a^2 Q_c^0 = +aQ\,,$$
$$\dot{\rho}_d + 3\mathcal{H}\left(1+\omega\right)\rho_d = a^2 Q_d^0 = -aQ\,.$$

$$Q = 3H(\lambda_1\rho_c + \lambda_2\rho_d)$$

$$\dot{\delta}_c = -(kv_c + \frac{\dot{h}}{2}) + 3\mathcal{H}\lambda_2\frac{1}{r}\left(\delta_d - \delta_c\right)\,,$$
$$\dot{\delta}_d = -\left(1+\omega\right)\left(kv_d + \frac{\dot{h}}{2}\right) + 3\mathcal{H}(\omega - c_e^2)\delta_d + 3\mathcal{H}\lambda_1 r\left(\delta_d - \delta_c\right) - 3\mathcal{H}\left(c_e^2 - c_a^2\right)\left[3\mathcal{H}\left(1+\omega\right) + 3\mathcal{H}\left(\lambda_1 r + \lambda_2\right)\right]\frac{v_d}{k}\,,$$
$$\dot{v}_c = -\mathcal{H}v_c - 3\mathcal{H}(\lambda_1 + \frac{1}{r}\lambda_2)v_c\,,$$
$$\dot{v}_d = -\mathcal{H}\left(1 - 3c_e^2\right)v_d + \frac{3\mathcal{H}}{1+\omega}\left(1+c_e^2\right)\left(\lambda_1 r + \lambda_2\right)v_d + \frac{kc_e^2\delta_d}{1+\omega}\,,$$

—— *arXiv: 1605.04138*

Interacting DE Model

- The *IDE* Model:

Model	Q	DE EoS	Constraints
I	$3\lambda_2 H\rho_d$	$-1 < \omega < 0$	$\lambda_2 < 0$
II	$3\lambda_2 H\rho_d$	$\omega < -1$	$0 < \lambda_2 < -2\omega\Omega_c$
III	$3\lambda_1 H\rho_c$	$\omega < -1$	$0 < \lambda_1 < -\omega/4$
IV	$3\lambda H\left(\rho_d + \rho_c\right)$	$\omega < -1$	$0 < \lambda < -\omega/4$

Parameters	Prior			
$\Omega_b h^2$	$[0.005, 0.1]$			
$\Omega_c h^2$	$[0.001, 0.99]$			
100θ	$[0.5, 10]$			
τ	$[0.01, 0.8]$			
n_s	$[0.9, 1.1]$			
$\log(10^{10}A_s)$	$[2.7, 4]$			
	Model I	Model II	Model III	Model IV
ω	$[-1, -0.3]$	$[-3, -1]$	$[-3, -1]$	$[-3, -1]$
λ	$[-0.4, 0]$	$[0, 0.4]$	$[0, 0.01]$	$[0, 0.01]$

—— *arXiv: 1605.04138*

21-cm Angular Power Spectrum

- The *Brightness Temperature Fluctuation* in 21cm Cosmology

$$\Delta_{T_{\rm b}}(z,\hat{\mathbf{n}}) = \delta_n - \frac{1}{\mathcal{H}}\left[\hat{\mathbf{n}}\cdot(\hat{\mathbf{n}}\cdot\vec{\nabla})\mathbf{v}\right] + \left(\frac{{\rm d}\ln(a^3\overline{n}_{\rm HI})}{{\rm d}\eta} - \frac{\dot{\mathcal{H}}}{\mathcal{H}} - 2\mathcal{H}\right)\delta\eta + \frac{1}{\mathcal{H}}\dot{\phi} + \psi$$

- *First Two Terms*: usual density fluctuation and redshift-space distortions (RSD)
- *The Third Term*: evaluating the zero-order brightness temperature at the perturbed time corresponding to the observed redshift
- *The Fourth Term*: ISW effect
- *The Fifth Term*: the conversion between radial distance in gas frame ($d\lambda$) with increments in redshift (dz) , i.e., $|d\lambda/dz|$.

21-cm Angular Power Spectrum

- Walk into the *Fourier space*

$$\begin{aligned}\Delta_{T_{\rm b},\ell}(\mathbf{k},z) &= \Delta^{(1)}_{T_{\rm b},\ell}(\mathbf{k},z)+\Delta^{(2)}_{T_{\rm b},\ell}(\mathbf{k},z)+\Delta^{(3)}_{T_{\rm b},\ell}(\mathbf{k},z)+\Delta^{(4)}_{T_{\rm b},\ell}(\mathbf{k},z)+\Delta^{(5)}_{T_{\rm b},\ell}(\mathbf{k},z)\\ &= \left(\tilde{\delta}_n+\frac{1}{\mathcal{H}}\dot{\tilde{\phi}}+\tilde{\psi}\right)j_\ell(k\chi)+\frac{1}{\mathcal{H}}\tilde{v}(\mathbf{k})kj''_\ell(k\chi)\\ &- \left(\frac{1}{\mathcal{H}}\frac{\mathrm{d}\ln(a^3\bar{n}_{\rm HI})}{\mathrm{d}\eta}-\frac{\dot{\mathcal{H}}}{\mathcal{H}^2}-2\right)\times\left[\tilde{\psi}j_\ell(k\chi)+\tilde{v}(\mathbf{k})j'_\ell(k\chi)+\int_0^\chi(\dot{\tilde{\phi}}+\dot{\tilde{\psi}})j_\ell(k\chi')\mathrm{d}\chi'\right] \quad (2.86)\end{aligned}$$

- *First Two Terms*: the intrinsic density fluctuation and RSD effect
- *The Third Term*: usual SW effect
- *The Fourth Term*: Doppler shift
- *The Fifth Term*: ISW contributions

21-cm Angular Power Spectrum

- The *IDE* Model:

$$\dot{v}_m = -aHv_m + k\psi - v_m \frac{a^2 Q_c^0}{\rho_m}$$

$$v_m = \frac{\rho_c v_c + \rho_b v_b}{\rho_c + \rho_b}$$

$$\Delta_{T_b,\ell}(\mathbf{k},z) = \Delta^{(1)}_{T_b,\ell}(\mathbf{k},z) + \Delta^{(2)}_{T_b,\ell}(\mathbf{k},z) + \Delta^{(3)}_{T_b,\ell}(\mathbf{k},z) + \Delta^{(4)}_{T_b,\ell}(\mathbf{k},z) + \Delta^{(5)}_{T_b,\ell}(\mathbf{k},z) + \Delta^{(6)}_{T_b,l}(\mathbf{k},z)$$

$$= \left(\tilde{\delta}_n + \frac{1}{\mathcal{H}}\dot{\tilde{\phi}} + \tilde{\psi}\right) j_\ell(k\chi) + \frac{1}{\mathcal{H}}\tilde{v}(\mathbf{k}) k j''_\ell(k\chi)$$

$$- \left(\frac{1}{\mathcal{H}}\frac{\mathrm{d}\ln(a^3\bar{n}_{\mathrm{HI}})}{\mathrm{d}\eta} - \frac{\dot{\mathcal{H}}}{\mathcal{H}^2} - 2\right) \times \left[\tilde{\psi} j_\ell(k\chi) + \tilde{v}(\mathbf{k}) j'_\ell(k\chi) + \int_0^\chi (\dot{\tilde{\phi}} + \dot{\tilde{\psi}}) j_\ell(k\chi')\mathrm{d}\chi'\right] \quad (2.86)$$

$$+ \tilde{v}_m(\mathbf{k}) \frac{a^2 Q_c^0}{\rho_m} j'_l(k\chi)$$

21-cm Angular Power Spectrum

- To calculate C_l :

$$C_l \sim (4\pi) \int dlnk \left(\frac{k^3}{2\pi^2}\right) < \Delta T_{b,l}(k,z) \Delta T^*_{b,l}(k,z) >$$

- The shot noise C_l^{shot}:

$$C_\ell^{\rm shot} = \bar{T}^2(z)/\bar{N}(z)$$

where $\bar{T}(z)$ is the HI background temperature, and $\bar{N}(z)$ is the angular density of sources.

$$\bar{T}(z) = 44\,\mu\mathrm{K}\left(\frac{\Omega_{\rm HI}(z)h}{2.45\times10^{-4}}\right)\frac{(1+z)^2}{E(z)},\qquad \bar{N}(z) = \frac{n_0 c}{H_0}\int\frac{r^2(z)}{E(z)}\mathrm{d}z.\qquad E(z) = H(z)/H_0.$$

- The thermal noise C_l^{therm}:

$$\sigma_{\rm t} = \frac{T_{\rm sys}}{\sqrt{t_{\rm pix}\Delta\nu}},\qquad C_l^{therm} \sim < \sigma_t \sigma_t^* >\qquad t_{\rm pix} = n_{\rm f} t_{\rm obs}\frac{\Omega_{\rm pix}}{\Omega_{\rm sur}},$$

where $\Delta\nu$ is the frequency channel width, $T_{\rm sys}$ is the system temperature, and $t_{\rm pix}$ is the integration time per beam defined by

where $n_{\rm f}$ denotes the number of feed horns, $t_{\rm obs}$ is the total integration time, $\Omega_{\rm sur}$ is the survey area, and $\Omega_{\rm pix} = \theta^2_{\rm FWHM}$ is the beam area.

21-cm Angular Power Spectrum

- Survey Configurations of BINGO and SKA1-MID :

	BINGO	SKA1-MID Band 1	SKA1-MID Band 2
Frequency range (MHz)	[980, 1260]	[350, 1050]	[950, 1405]
Redshift range	[0.13, 0.48]	[0.35, 3.06]	[0.01, 0.49]
System temperature $T_{\rm sys}$ (K)	70	Eq. 23	15
Number of dishes $n_{\rm d}$	1	197	197
Number of beams $n_{\rm beam}$ (dual pol.)	50×2	1×2	1×2
Illuminated aperture $D_{\rm dish}$ (m)	25	15	15
Beam resolution $\theta_{\rm FWHM}$ (arcmin)	40	117.9	70
Sky coverage $\Omega_{\rm sur}$ (deg^2)	3000	20000	5000
Observation time $t_{\rm obs}$ (yr)	1	1.14	1.14
Bandwidth $\delta\nu$ (MHz)	8.75	8.75	8.75
Number of channels $N_{\rm bin}$	32	80	52

21-cm Angular Power Spectrum

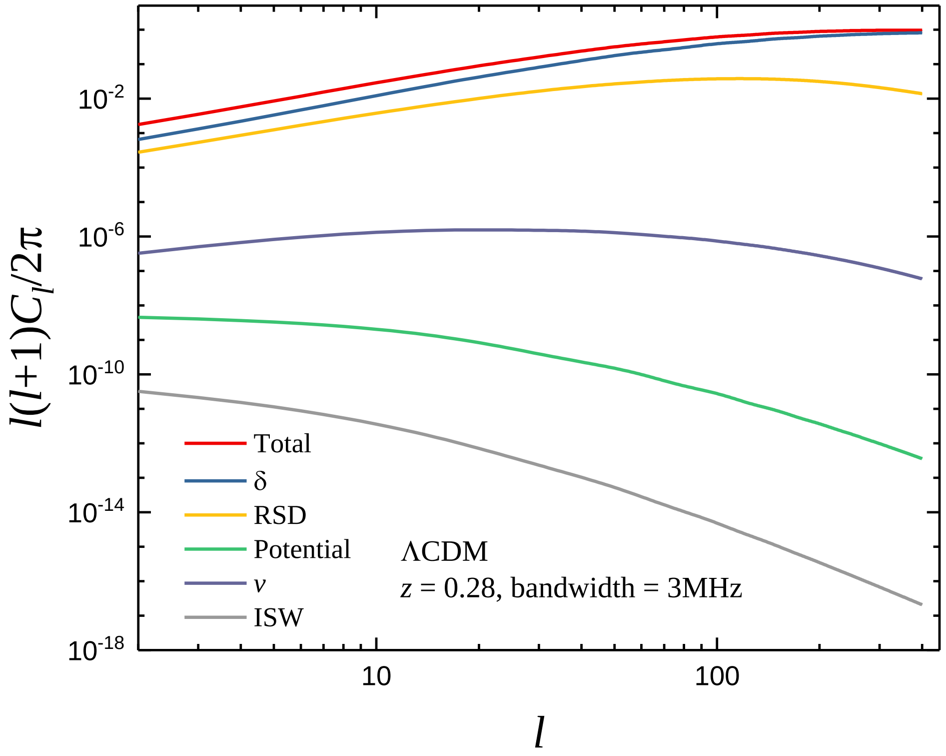

(a)

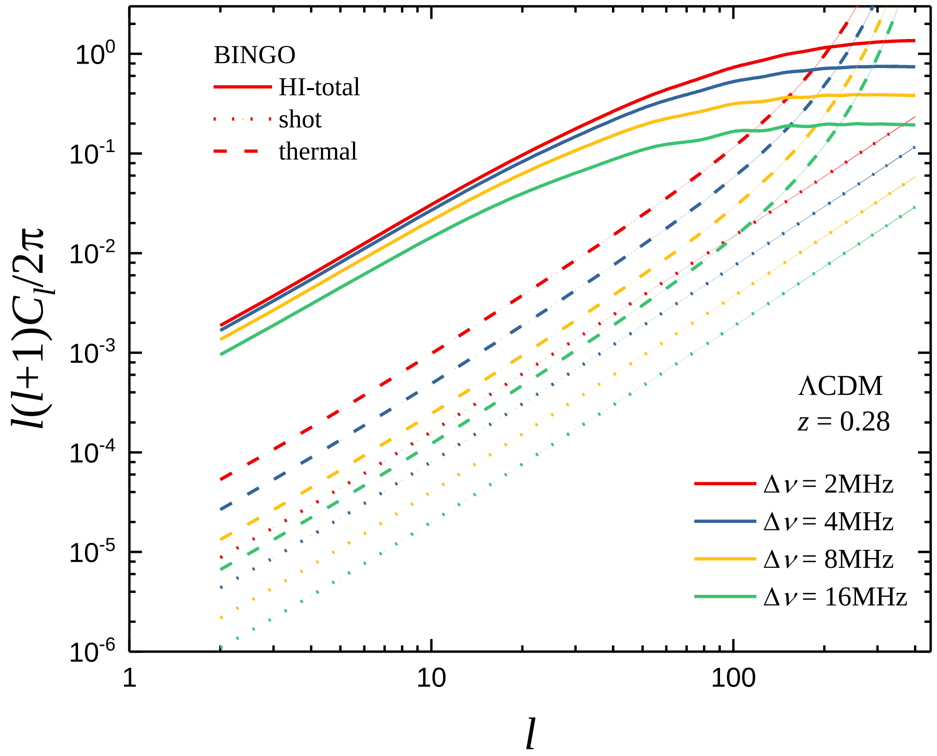

(b)

- The predicted 21-cm C_l power spectra of ΛCDM after Planck 2018 at $z = 0.28$ with bandwidth $= 3\text{MHz}$. (a) The two major contributions are from overdensity and RSD, which are much more prominent than those from Doppler, SW and ISW effects. (b) The signal and noise level with respect to different bandwidths. Narrowing bandwidth can both enhance the signal and noise level.

21-cm Angular Power Spectrum

- Signal and Noise:

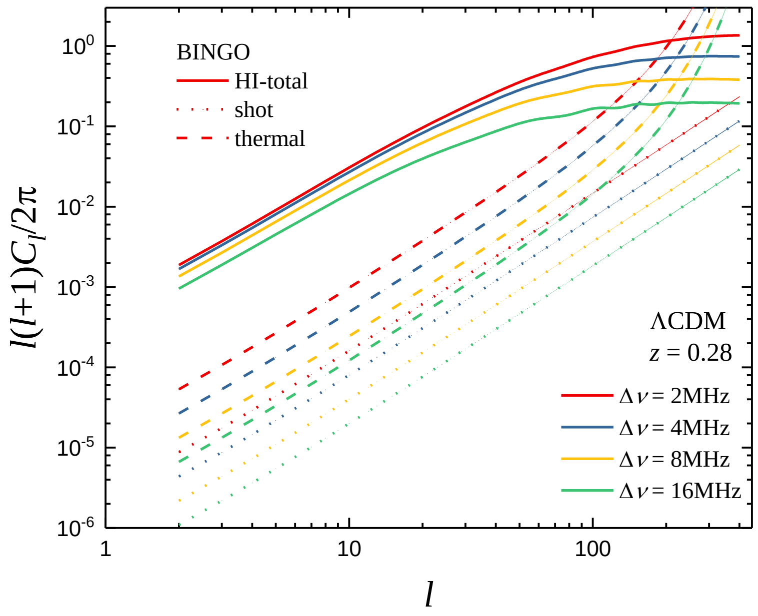

(a)

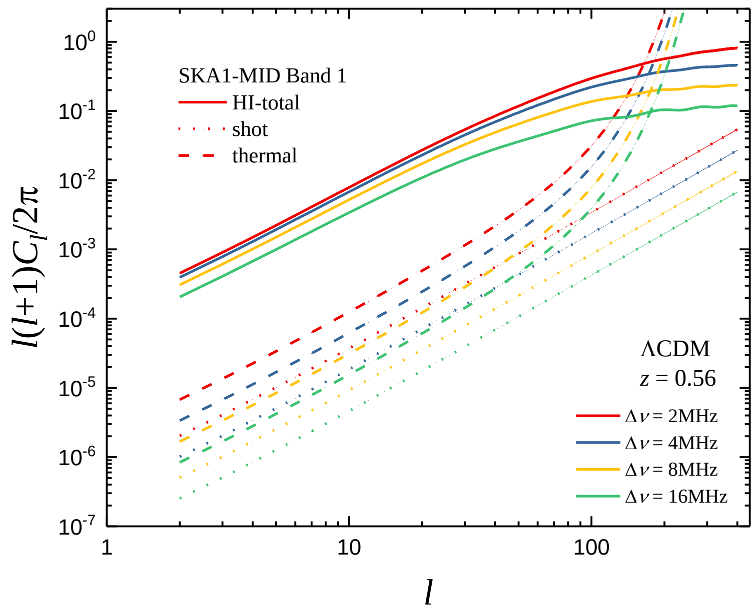

(b)

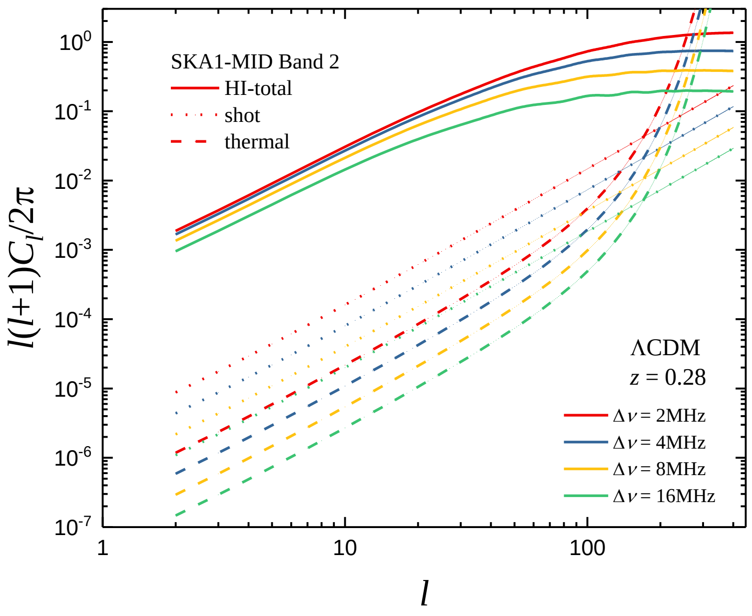

(c)

- Signals in contrast to shot / thermal noises with respect to different bandwidths for three HI IM projects, BINGO, SKA1-MID Band 1 and Band 2, respectively.

Xiao et al. (in prep).

21-cm Angular Power Spectrum

- If we vary *w* …

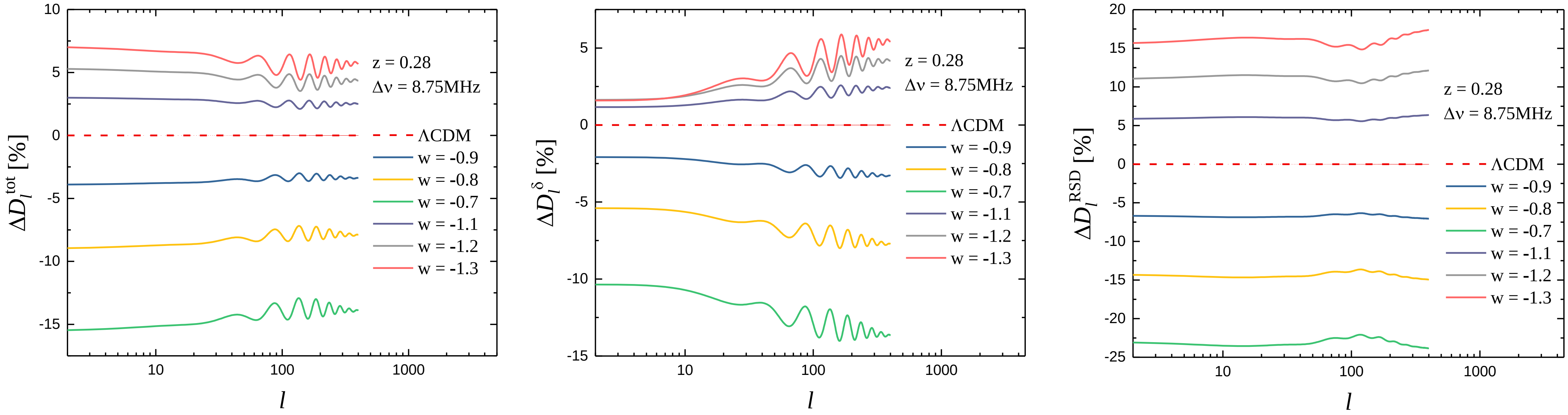

(a) (b) (c)

- The effects of w on C_ls of total contribution, intrinsic overdensity and RSD, respectively in wCDM. Basically the level of signals decreases with w.

*$D_l^i = l(l+1)C_l^i$ and $\Delta D_l^i = (D_l^i - D^{i}_{l,\Lambda CDM}) / D^{i}_{l,\Lambda CDM}$

Xiao et al. (in prep).

21-cm Angular Power Spectrum

- How to understand such discrepancies?

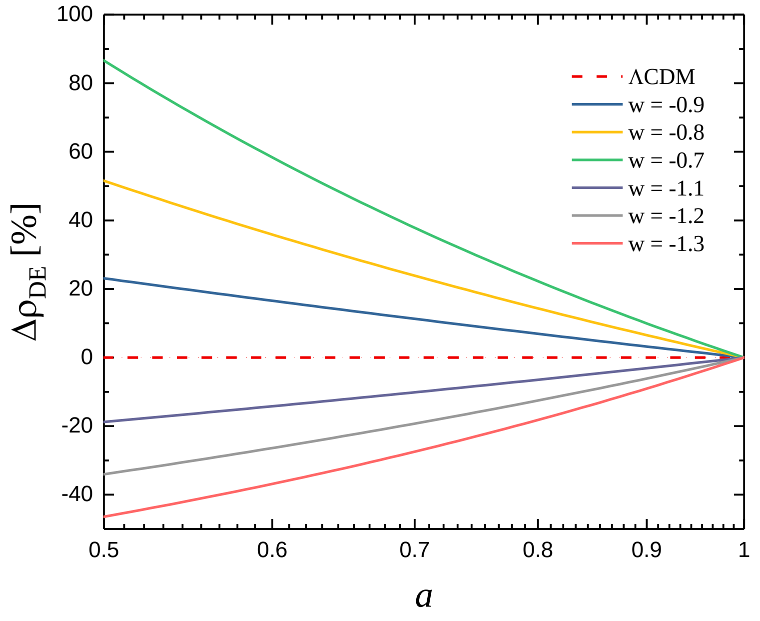

(a)

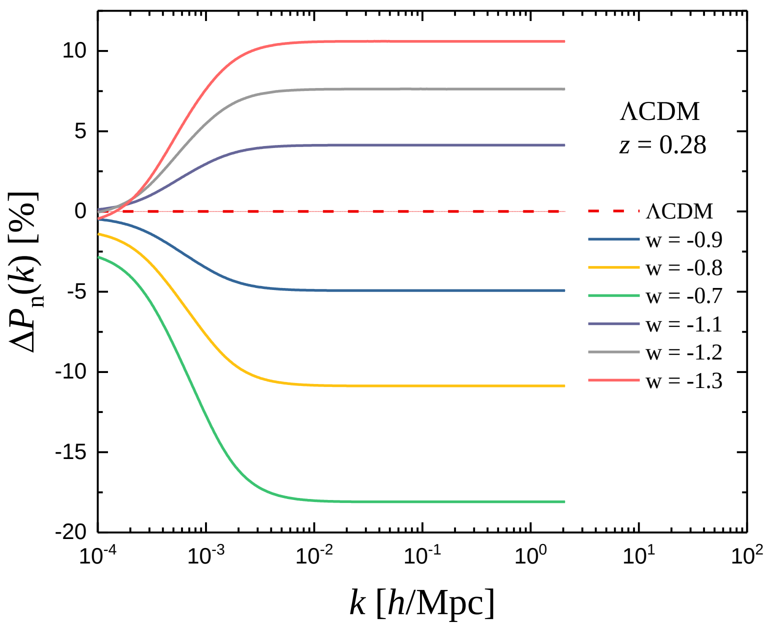

(b)

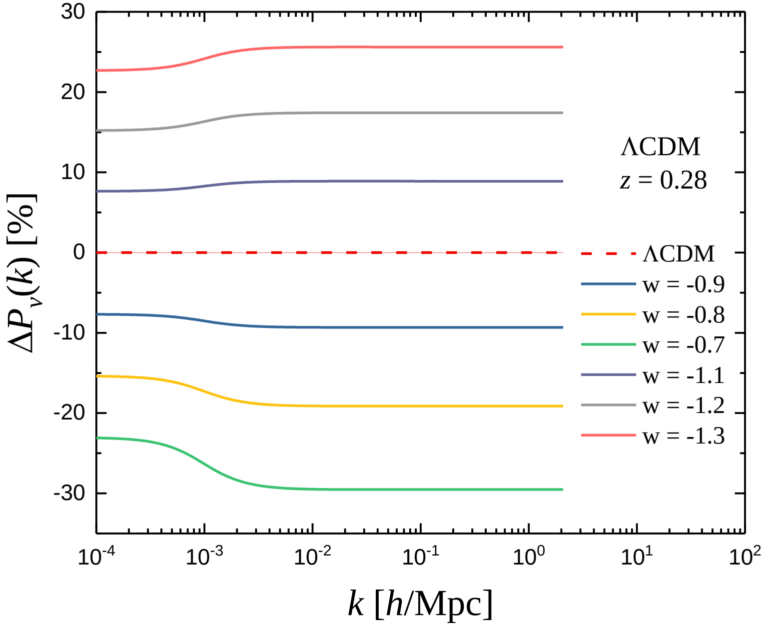

(c)

- On a fixed redshift, the DE density increases with w. In wCDM model, if we fix the evolution of matter components, more DE prefers to suppress the matter condense and the gravity-induced peculiar velocity.

$*\Delta A = (A - A_{\Lambda CDM}) / A_{\Lambda CDM}$

Xiao et al. (in prep).

21-cm Angular Power Spectrum

- For *IDE* I ($Q \propto \rho_{DE}$), varying λ_2

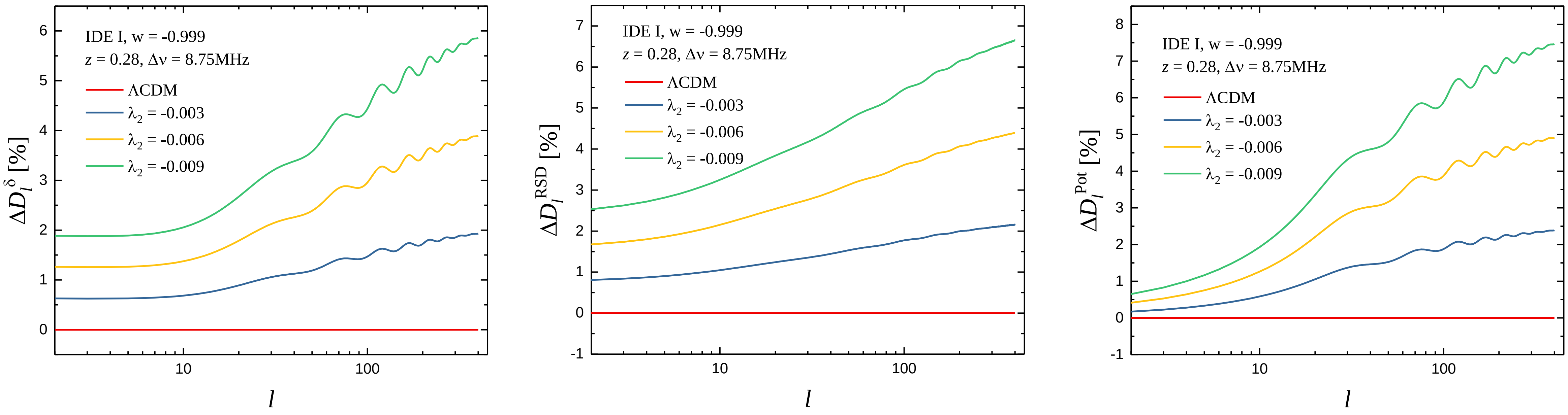

(a) (b) (c)

- In IDE I the energy flow is from DM to DE, indicating more DM and less DE in the past, and thus the 21-cm signals get enhanced. Also worth noting that, the signal increments are more significant on small scales.

Xiao et al. (in prep).

21-cm Angular Power Spectrum

- For *IDE* I ($Q \propto \rho_{DE}$), varying λ_2

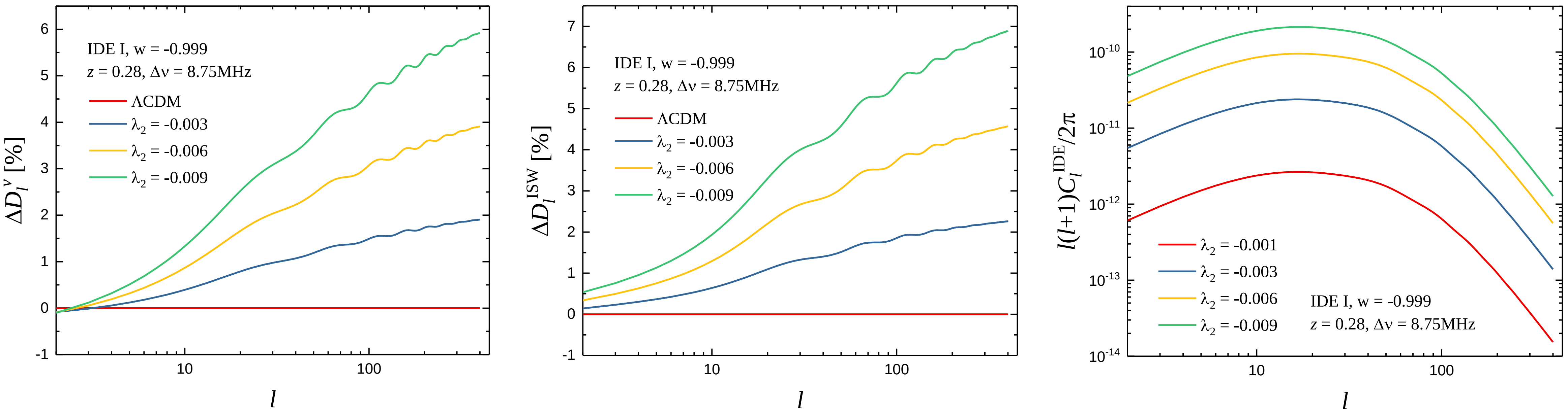

(a) (b) (c)

- The change to each decomposed signal from IDE shows similar scale dependence. In terms of its magnitude, the IDE extra contribution to the 21-cm signal is negligible.

Xiao et al. (in prep).

21-cm Angular Power Spectrum

- For *IDE* IV ($Q \propto \rho_{DM} + \rho_{DE}$), varying λ

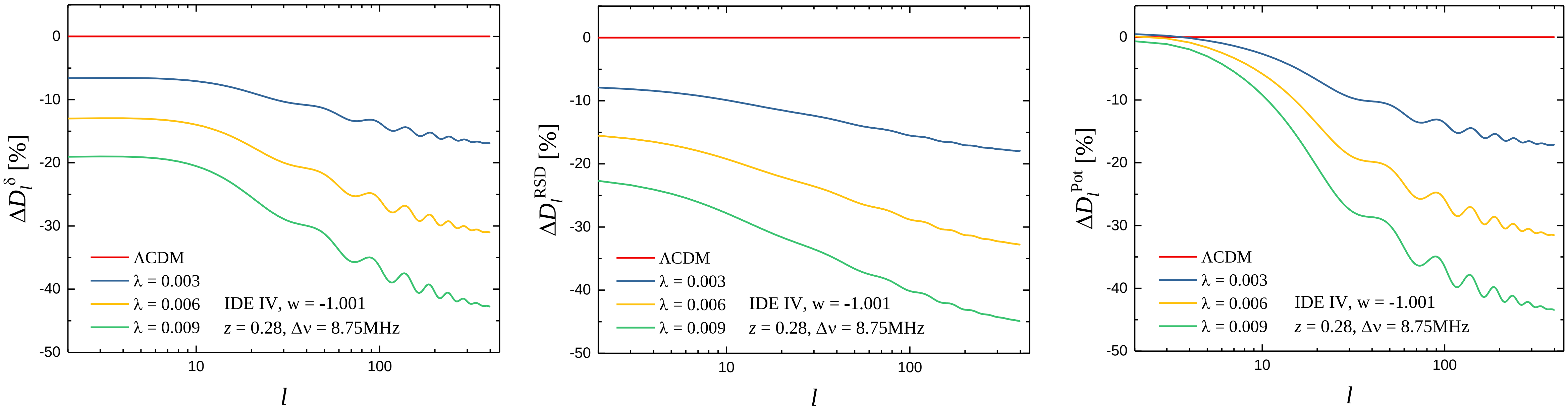

(a) (b) (c)

- Whilst IDE IV behaves opposite to IDE I, the mechanism behind is the same.

Xiao et al. (in prep).

21-cm Angular Power Spectrum

- For *IDE* IV ($Q \propto \rho_{DM} + \rho_{DE}$), varying λ

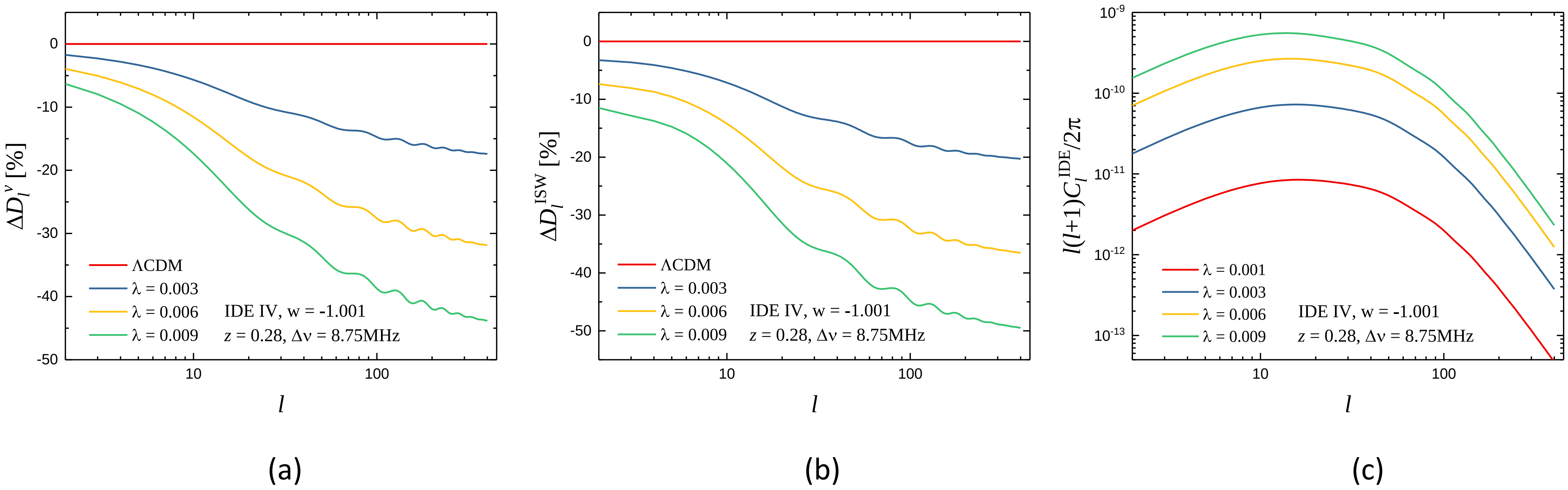

- However, against IDE I, the 21-cm signals in IDE IV are extremely sensitive to an interaction $\propto \rho_{DM} + \rho_{DE}$.

Xiao et al. (in prep).

Fisher Matrix Analysis

- The *Fisher Matrix*:

$$F_{ij} = \sum_{\ell=2}^{\ell_{\rm max}} \sum_{XX',YY'} \frac{\partial C_\ell^{XX'}}{\partial \theta_i} [{\rm Cov}(XX',YY')]_\ell^{-1} \frac{\partial C_\ell^{YY'}}{\partial \theta_j},$$

$$[{\rm Cov}(XX',YY')]_\ell = \frac{1}{(2\ell+1) f_{\rm sky}} \left(\hat{C}_\ell^{XY} \hat{C}_\ell^{X'Y'} + \hat{C}_\ell^{XY'} \hat{C}_\ell^{X'Y} \right),$$

$$\hat{C}_\ell(z_i,z_j) = C_\ell^{\rm HI}(z_i,z_j) + \delta(z_i,z_j) C_\ell^{\rm shot} + N_\ell(z_i,z_j) B_\ell(z_i,z_j),$$

$$\boldsymbol{\theta} = \{\Omega_b h^2, \Omega_c h^2, w, h, n_s, \log(10^{10} A_s), b_{\rm HI}, \lambda_1, \lambda_2\}.$$

$$N_\ell(z_i,z_j) = \left(\frac{4\pi}{N_{\rm pix}}\right) \sigma_{\rm T,i} \sigma_{\rm T,j},$$

$$\sigma_{b,i} = \theta_{\rm B}(z_i)/\sqrt{8 \ln 2}$$

$$\theta_{\rm B}(z_i) = \theta_{\rm FWHM}(\nu_{\rm med}) \frac{\nu_{\rm med}}{\nu_i}.$$

$$B_\ell(z_i,z_j) = \exp\left[\ell^2 \sigma_{\rm b,i} \sigma_{\rm b,j}\right].$$

Fisher Matrix Analysis

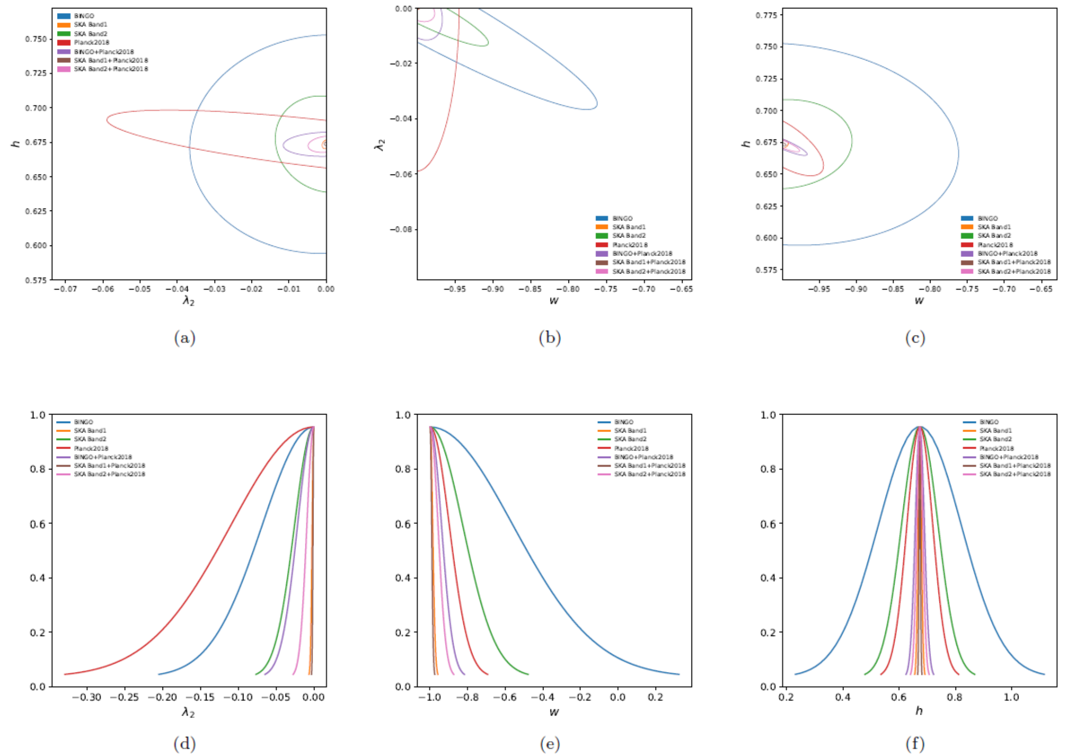

Figure 9. The forecasted 2D and 1D distributions of λ_2, w and h in case of IDE 1. SKA1-MID shows its remarkable strength in parameter constraints, and both HI IM projects have advantages on laying bounds to the interacting strength over *Planck* 2018.

- For *IDE* I ($Q \propto \rho_{DE}$):
  a) The capability of SKA1-MID Band1 in constraining λ_2, w and h is even above Planck 2018
  b) All three HI IM projects can lay tighter constraints on the interacting strength than the CMB measurement to date
  c) Planck 2018 still holds its advantage on restricting early-universe parameters, i.e., A_s and n_s
  d) HI IM surveys are able to break the degeneracy between w and h resided in Planck data, thanks to their wide observing range of redshifts

Parameters	$\Omega_b h^2$ [0.02237]	$\Omega_c h^2$ [0.12]	w [-0.999]	$\log(10^{10} A_s)$ [3.044]	n_s [0.9649]	λ_2 [0.00]	h [0.6736]	b_{HI} [1.00]
BINGO alone	±0.0115	±0.0368	±0.3119	±0.3045	±0.0726	±0.0483	±0.1044	±0.1009
SKA B 1 alone	±0.00067	±0.0028	±0.0097	±0.0259	±0.0106	±0.0015	±0.0043	±0.0074
SKA B 2 alone	±0.0055	±0.0142	±0.1228	±0.1075	±0.0247	±0.0180	±0.0461	±0.0405
Planck	±0.00015	±0.0334	±0.0722	±0.0163	±0.0045	±0.0776	±0.0326	...
BINGO+*Planck*	±0.00013	±0.0060	±0.0429	±0.0160	±0.0039	±0.0152	±0.0116	±0.0187
SKA B 1+*Planck*	±0.00011	±0.00085	±0.0058	±0.0102	±0.0025	±0.0007	±0.0018	±0.0062
SKA B 2+*Planck*	±0.00013	±0.0030	±0.0296	±0.0157	±0.0036	±0.0064	±0.0078	±0.0121

Table 3. The projected 1σ uncertainties for IDE 1 from BINGO, SKA1-MID Bnad 1 and Band 2 respectively via Fisher matrix forecast and *Planck* 2018 through CosmoMC runs, and also their joint results by adding up each Fisher matrix. Square brackets in the *1st row* are the parameter fiducial values declared in Sec. 1.

Xiao et al. (in prep).

Fisher Matrix Analysis

- For *IDE* II ($Q \propto \rho_{DE}$):

Parameters	$\Omega_b h^2$ [0.02237]	$\Omega_c h^2$ [0.12]	w [-1.001]	$\log(10^{10}A_s)$ [3.044]	n_s [0.9649]	λ_2 [0.00]	h [0.6736]	$b_{\rm HI}$ [1.00]
BINGO alone	±0.0115	±0.0368	±0.3131	±0.3055	±0.0723	±0.0484	±0.1044	±0.1011
SKA B 1 alone	±0.00064	±0.0028	±0.0075	±0.0262	±0.0105	±0.0016	±0.0047	±0.0074
SKA B 2 alone	±0.0054	±0.0142	±0.1227	±0.1073	±0.0248	±0.0180	±0.0460	±0.0403
Planck	±0.00015	±0.009	±0.2589	±0.0158	±0.0043	±0.0257	±0.0907	...
BINGO+*Planck*	±0.00014	±0.0050	±0.0503	±0.0155	±0.0039	±0.0136	±0.0138	±0.0169
SKA B 1+*Planck*	±0.00012	±0.00081	±0.0049	±0.0101	±0.0027	±0.00077	±0.0018	±0.0061
SKA B 2+*Planck*	±0.00013	±0.0026	±0.0337	±0.0153	±0.0035	±0.0062	±0.0083	±0.0112

Table 4. Same as the projected uncertainties listed in Tab. 3, while for IDE 2.

- Towards *IDE* II ~ IV:
  a) In terms of the forecast for HI IM surveys, IDE II are highly in line with IDE I, whereas IDE III well resembles IDE IV
  b) When $Q \propto \rho_{DM}$ or $Q \propto \rho_{DM} + \rho_{DE}$, BINGO's performance is fairly close to Planck in bounding w but inferior in interacting strength constraints

Xiao et al. (in prep).

Fisher Matrix Analysis

- For *IDE* III ($Q \propto \rho_{DM}$):

Parameters	$\Omega_b h^2$ [0.02237]	$\Omega_c h^2$ [0.12]	w [-1.001]	$\log(10^{10} A_s)$ [3.044]	n_s [0.9649]	λ_1 [0.00]	h [0.6736]	$b_{\rm HI}$ [1.00]
BINGO alone	±0.0120	±0.0650	±0.1062	±0.2966	±0.0836	±0.0137	±0.1079	±0.1107
SKA B1 alone	±0.00037	±0.0033	±0.0037	±0.0410	±0.0155	±0.0016	±0.0048	±0.0074
SKA B2 alone	±0.0055	±0.0224	±0.0511	±0.1079	±0.0263	±0.0043	±0.0474	±0.0388
Planck	±0.00018	±0.0036	±0.405	±0.0161	±0.0049	±0.0013	±0.1071	...
BINGO+*Planck*	±0.00017	±0.0014	±0.0685	±0.0153	±0.0038	±0.00063	±0.0133	±0.0160
SKA B1+*Planck*	±0.00012	±0.00096	±0.0035	±0.0111	±0.0034	±0.00032	±0.0018	±0.0065
SKA B2+*Planck*	±0.00016	±0.0012	±0.0392	±0.0144	±0.0035	±0.00052	±0.0079	±0.0125

Table 5. Same as the projected uncertainties given in Tab. 4, while for IDE 3.

- For *IDE* IV ($Q \propto \rho_{DM} + \rho_{DE}$):

Parameters	$\Omega_b h^2$ [0.02237]	$\Omega_c h^2$ [0.12]	w [-1.001]	$\log(10^{10} A_s)$ [3.044]	n_s [0.9649]	λ [0.00]	h [0.6736]	$b_{\rm HI}$ [1.00]
BINGO alone	±0.0122	±0.0797	±0.1630	±0.3239	±0.0866	±0.0174	±0.1105	±0.1670
SKA B1 alone	±0.00038	±0.0031	±0.0053	±0.0342	±0.0137	±0.0010	±0.0045	±0.0074
SKA B2 alone	±0.0055	±0.0257	±0.0686	±0.1136	±0.0262	±0.0053	±0.0478	±0.0535
Planck	±0.00019	±0.004	±0.389	±0.0166	±0.005	±0.0013	±0.1074	...
BINGO+*Planck*	±0.00017	±0.0016	±0.0696	±0.0157	±0.0040	±0.00069	±0.0133	±0.0166
SKA B1+*Planck*	±0.00013	±0.0011	±0.0036	±0.0113	±0.0035	±0.00033	±0.0018	±0.0065
SKA B2+*Planck*	±0.00016	±0.0014	±0.0407	±0.0148	±0.0037	±0.00058	±0.0079	±0.0132

Table 6. Same as the projected uncertainties shown in Tab. 5, while for IDE 4.

Xiao et al. (in prep).

Conclusions & Prospective

- *Density fluctuation* and *RSD* are the two leading terms among the contributions to the total 21-cm signal.
- Besides an extra term, $v_m a^2 Q_c^0/\rho_m$, the interaction will leave marks on every component of the brightness temperature fluctuation.
- The equation of state w plays a similar role in *IDE* scenarios as it does in ΛCDM, and thus the influence from the *interaction* is easily identified, especially on small scales.
- *More* DM and/or *less* DE during the cosmic expansion prefer to *enhance* every decomposition of the 21-cm signal, except for the extra IDE contribution which is propotional to the strength of the interaction.
- Compared with Planck 2018, both BINGO and SKA1-MID are with great potential in constraining w, h and the strength of the interaction.
- HI IM surveys are *promising* to facilitate the measurements of cosmological parameters and deepen our understanding of the late-time accelerated expansion, e.g., by opting for cross-correlating with the dataset from conventional galaxy surveys.


Thank You

Conclusions & Prospectives

- $\mathcal{Density\ fluctuation}$ and $\mathcal{RSD}$ are the two leading components of the total 21cm C_ls.
- In addition to an extra term, $v_m \frac{a^2 Q_c^0}{\rho_m}$, the interaction will leave some marks on every component of the brightness temperature fluctuation.
- The equation of state w plays a similar role in the $\mathcal{IDE}$ scenario as it does in ΛCDM, and thus the effects from the *interaction* is easily identified, especially those on small scales.
- *More* DM and/or *less* DE during the cosmic expansion prefer to *enhance* every component of the 21cm signals, except for the extra IDE contribution which is proportional to the strength of the interaction.
- The power of *BINGO* alone on parameter constraints is much weaker than that of *Planck*.
- Including *RSD* or narrowing the *bandwidth* is beneficial for a tighter constraint.

Some C_l Results

- For *IDE* I , varying w:

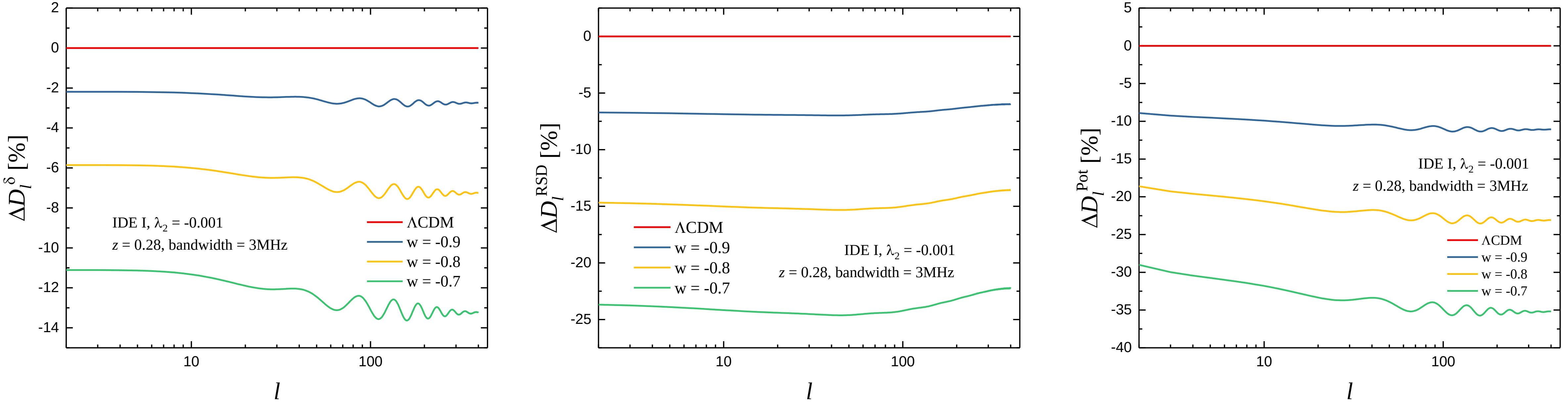

(a) (b) (c)

Figure 5 In IDE I (DM⇒DE), the effects from varying w are almost the same as one see in wCDM model.

Some C_l Results

- For *IDE* I, varying w:

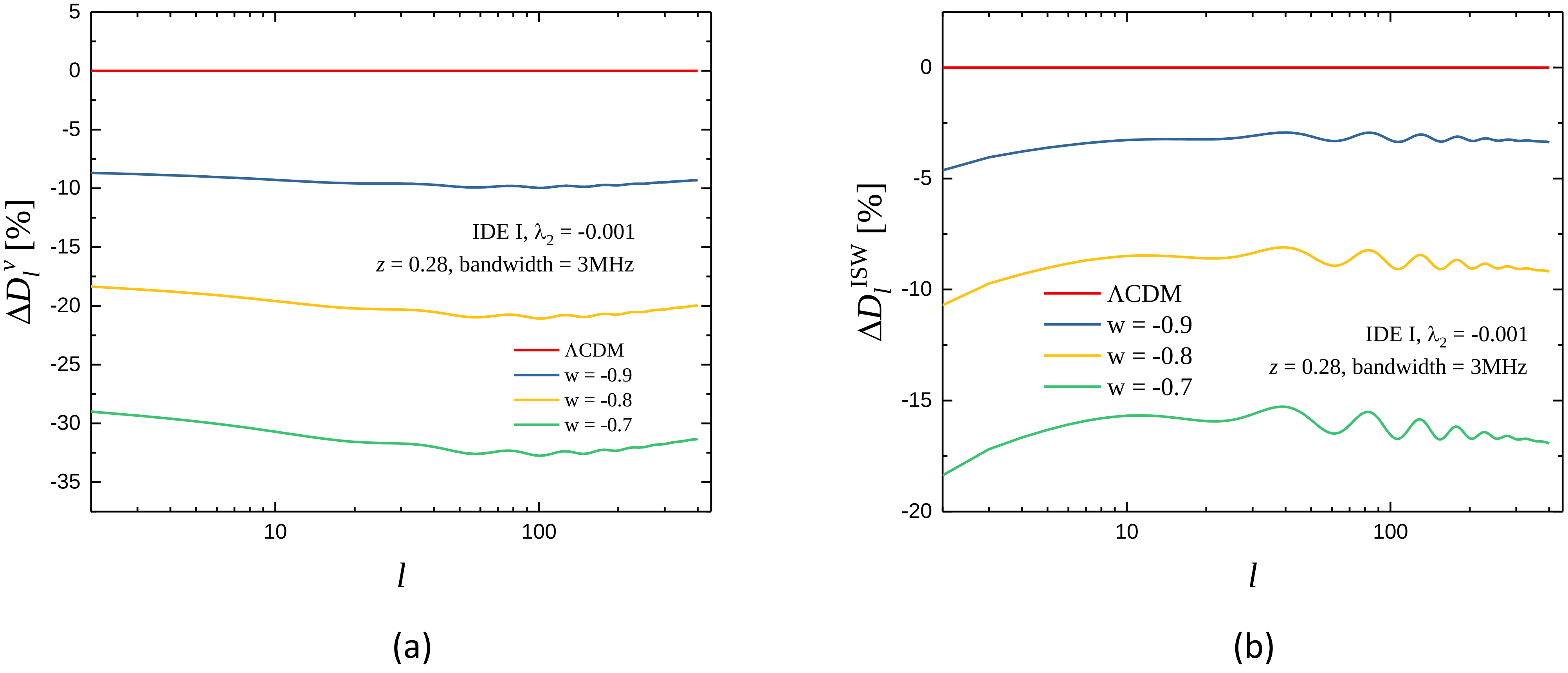

Figure 6 Similar to Fig.5, but for the Doppler and ISW effects.

Some C_l Results

- For *IDE* I, varying w:

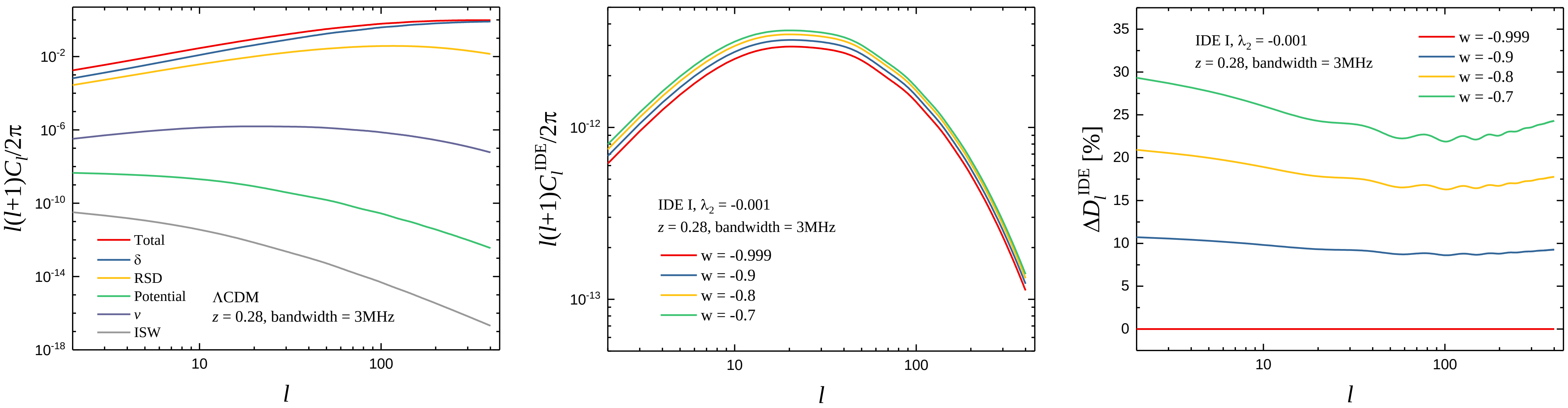

(a) (b) (c)

Figure 7 The 21cm signal from the extra IDE term in IDE I (DM⇒DE), of which the magnitude is on the level of the ISW contribution.

Some C_l Results

- For $\mathcal{IDE}$ IV, varying w:

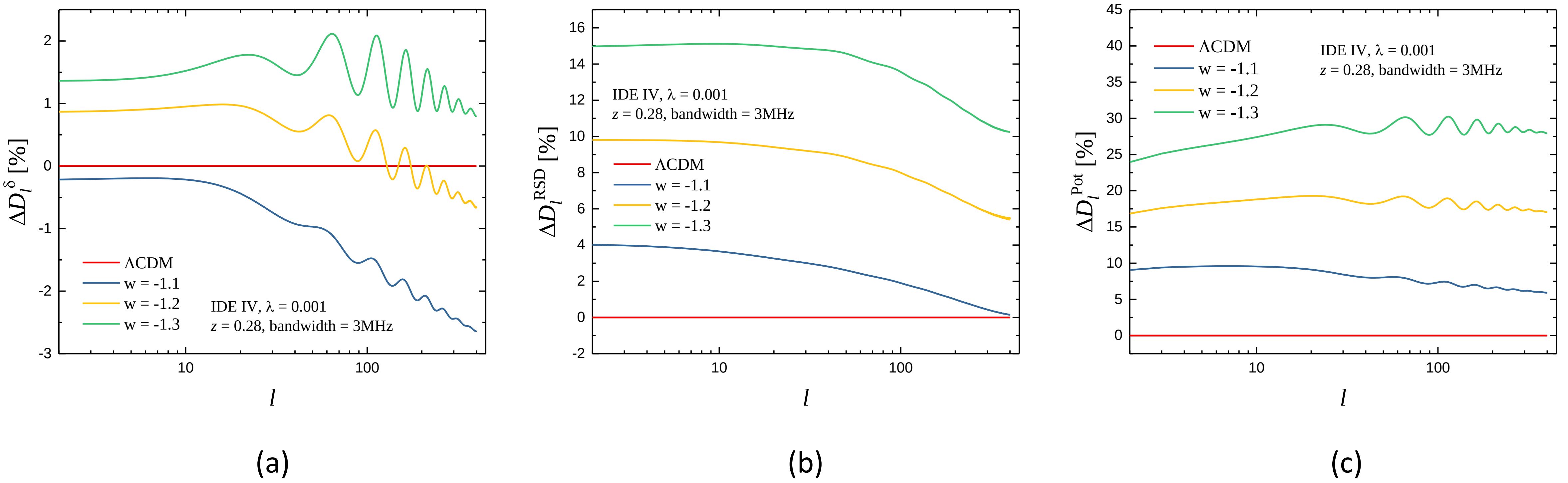

Figure 8 Same as the spectra discrepancies in Fig. 5, but for the case of IDE IV (DE⇒DM). Comparing with the wCDM pattern, we see a sharp decline on small scales.

Some C_l Results

- For *IDE* IV, varying w:

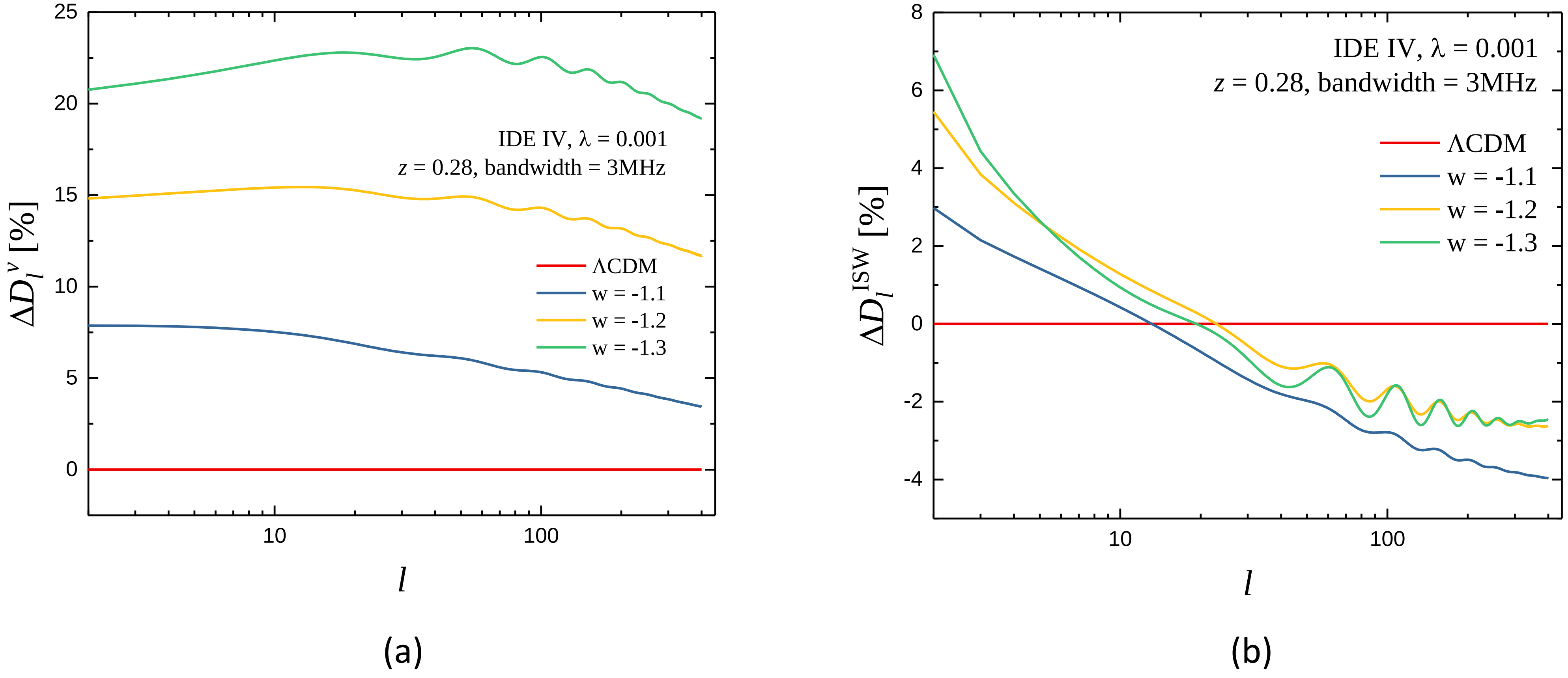

Figure 9 Similar to Fig. 8, but for the Doppler and ISW effects.

Some C_l Results

- For *IDE* IV, varying w:

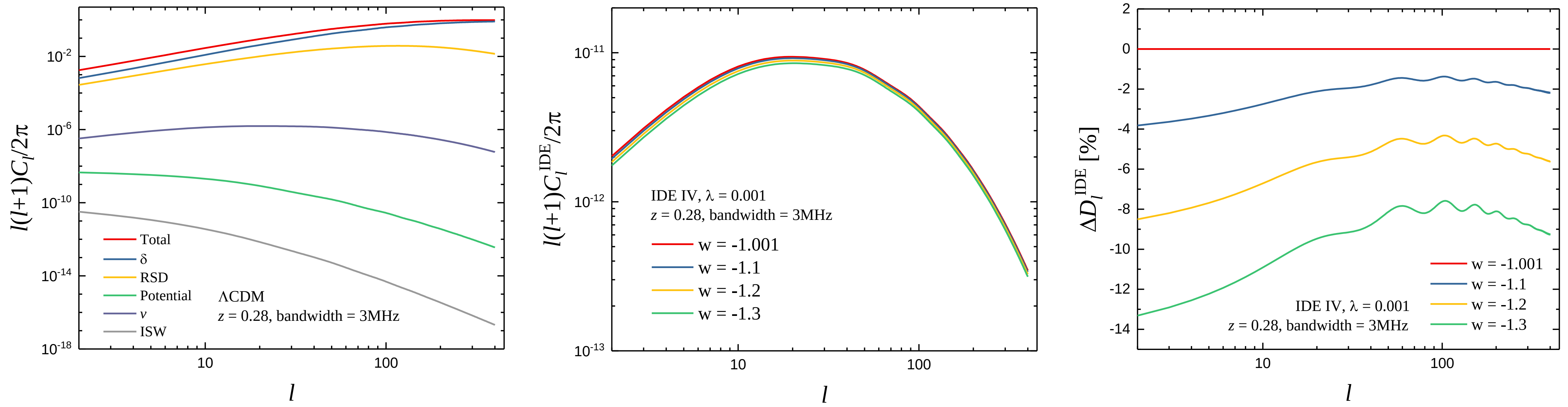

(a) (b) (c)

Figure 10 The 21cm signal from the extra IDE term in IDE IV (DE⇒DM), of which the magnitude is similar to the one in IDE I in condition of a same interacting strength.

Some C_l Results

- What happened in *IDE* IV?

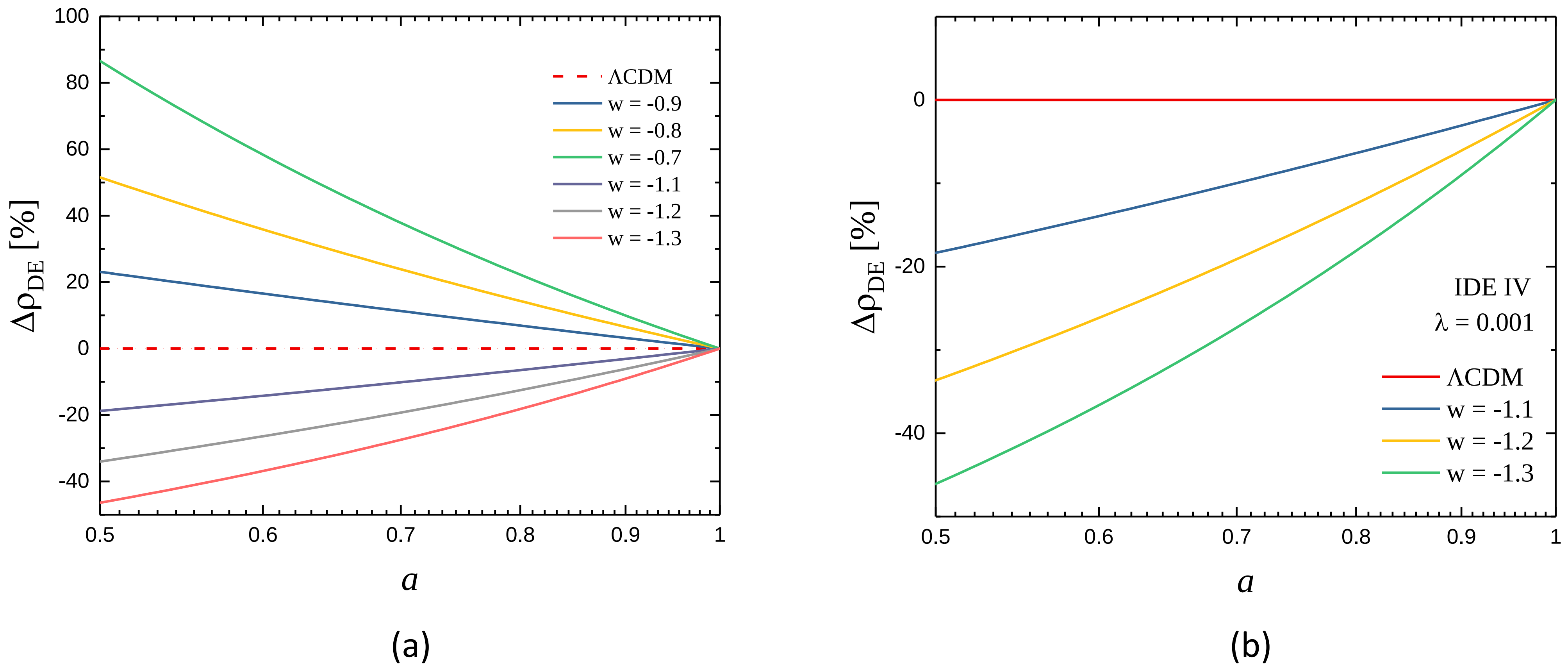

Figure 11 On background level, it seems nothing special, except for the tiny energy transfer from DE to DM.

Some C_l Results

- What happened in *IDE* IV?

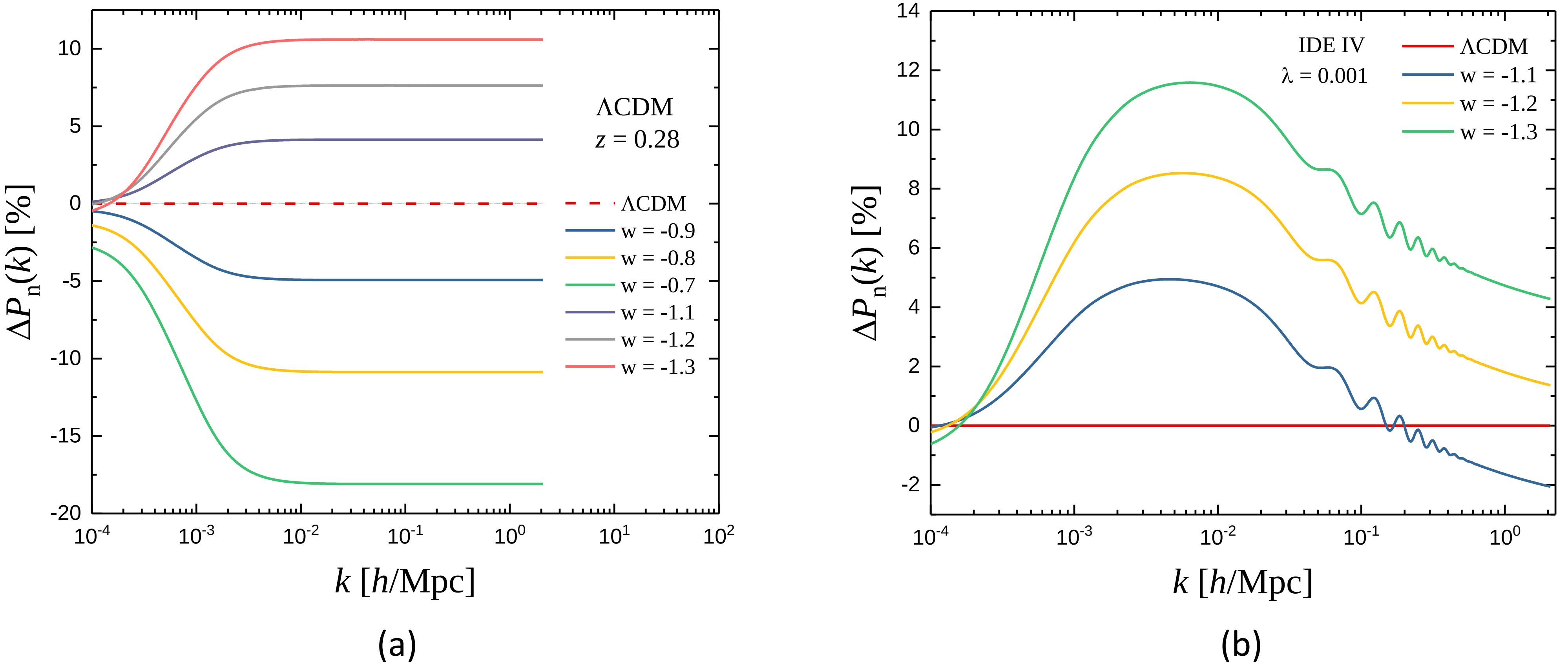

Figure 12 While on the level of perturbation, the power suppression on the high-k end is rather prominent. Note that, in IDE IV the interaction is tightly constrained by Planck and other data, which means this scenario is very sensitive to λ.

Some C_l Results

- What happened in *IDE* IV?

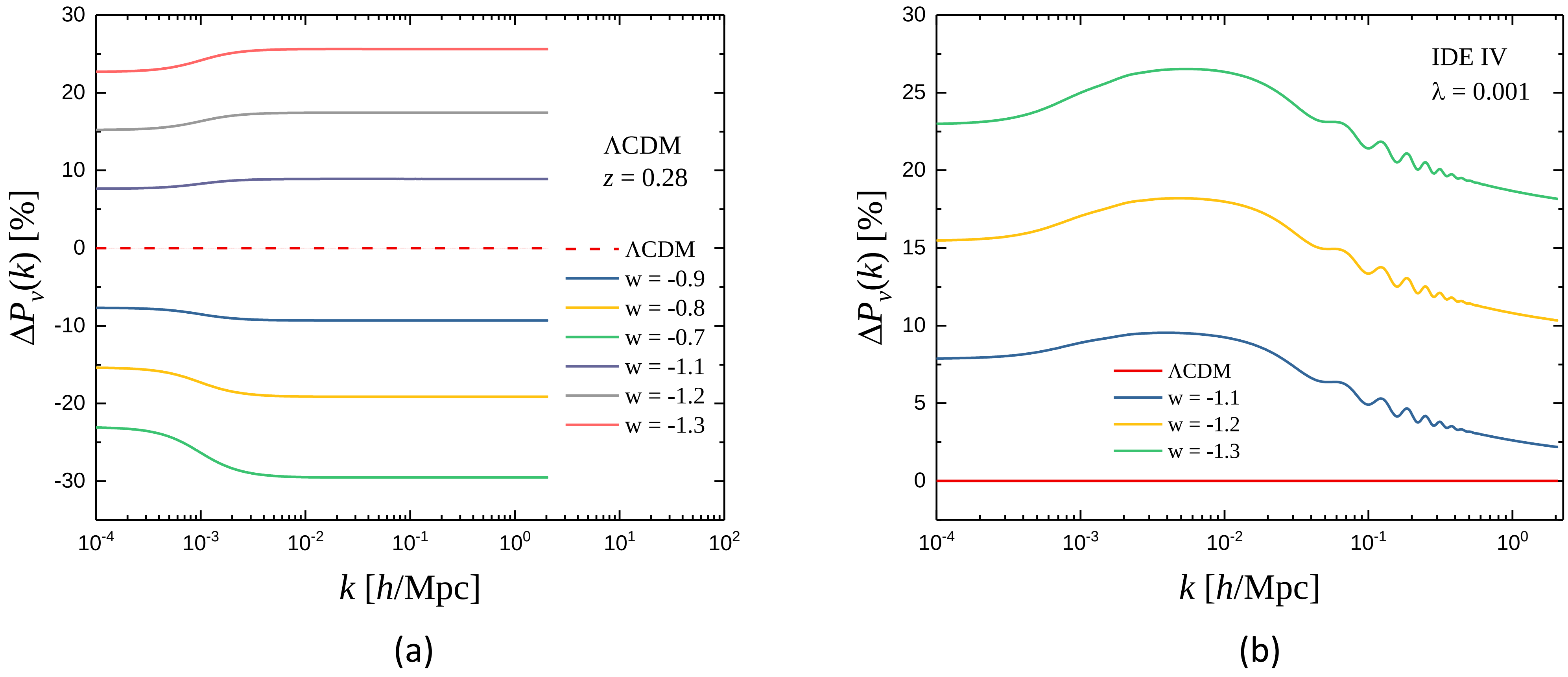

Figure 13 Same as the illustration in Fig. 12, but for the velocity power spectrum.

Some C_l Results

- For *IDE* IV, varying λ:

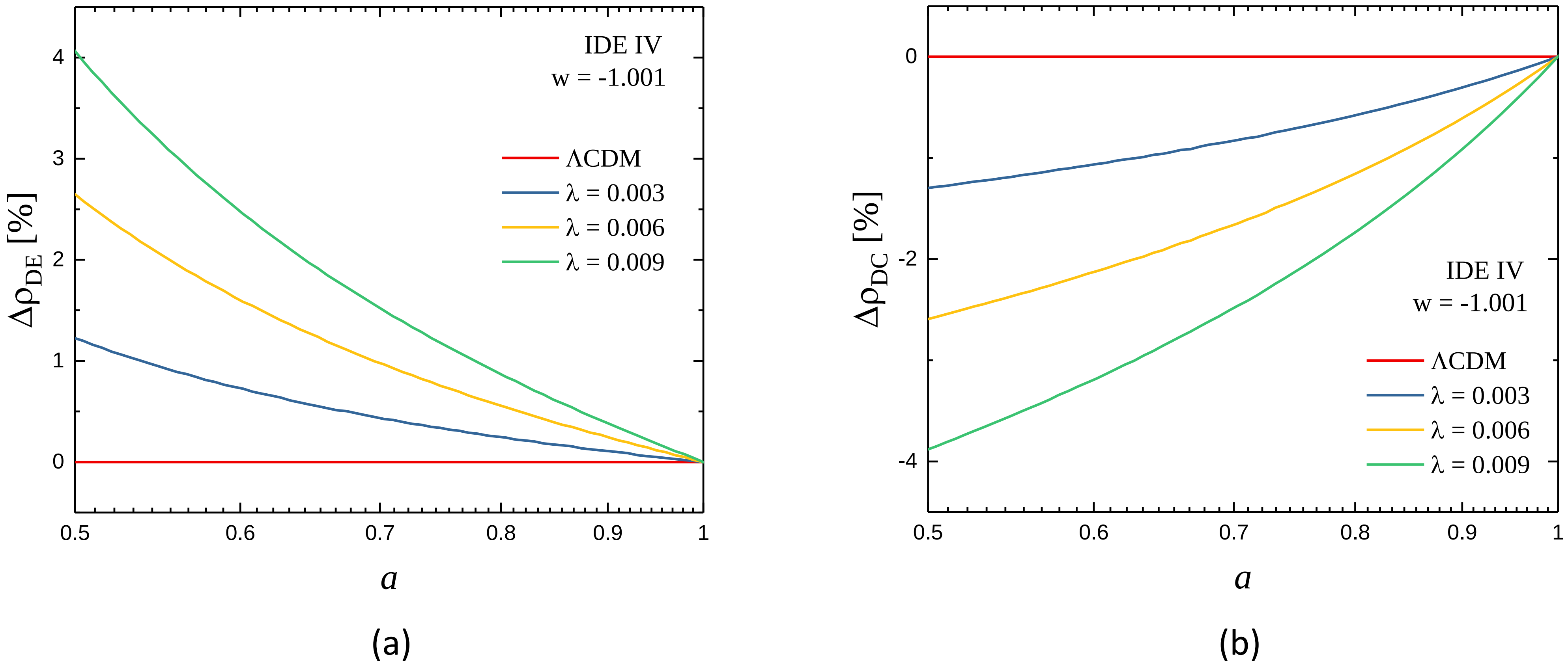

Figure 14 Fixing *w* close to ΛCDM, for checking the effects from the interaction independently.

Some C_l Results

- For *IDE* IV, varying λ:

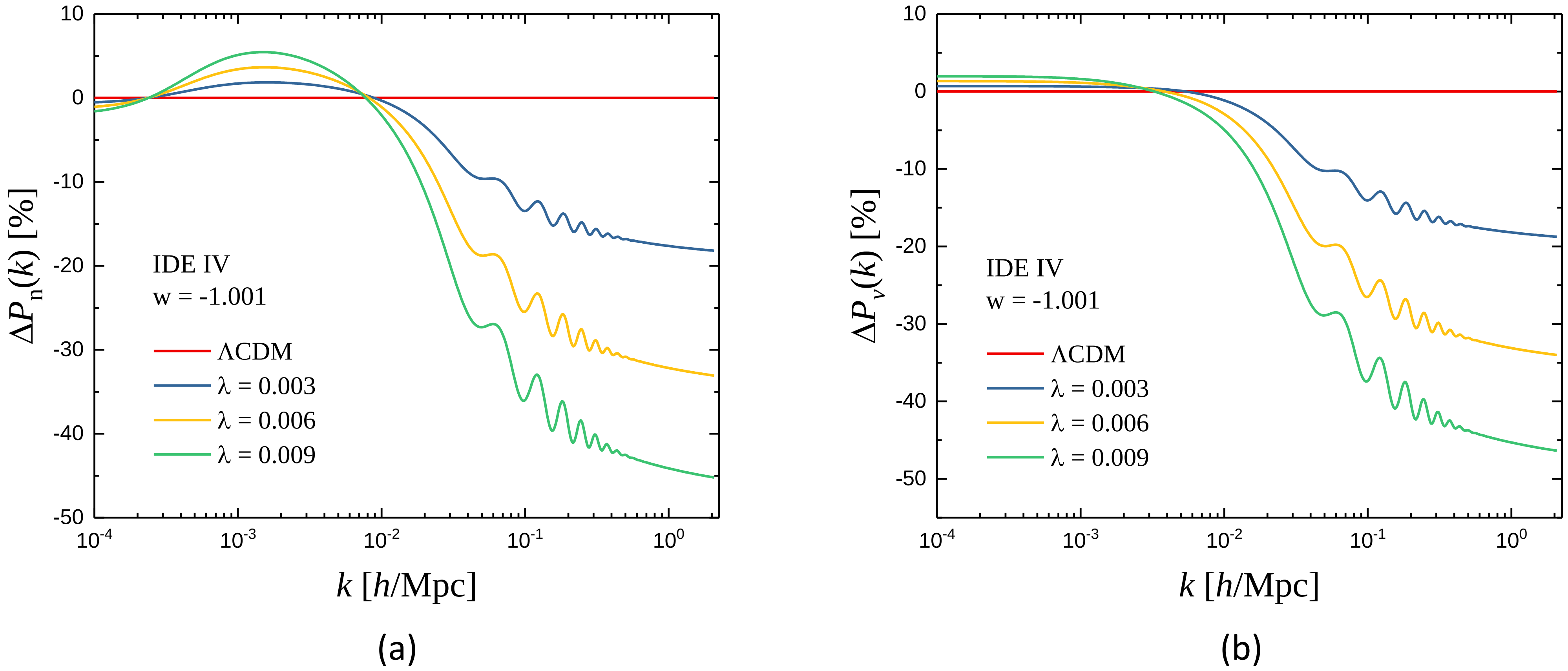

Figure 15 λ's influence on the power spectra of overdensity and peculiar velocity.

Some C_l Results

- For *IDE* IV, varying λ:

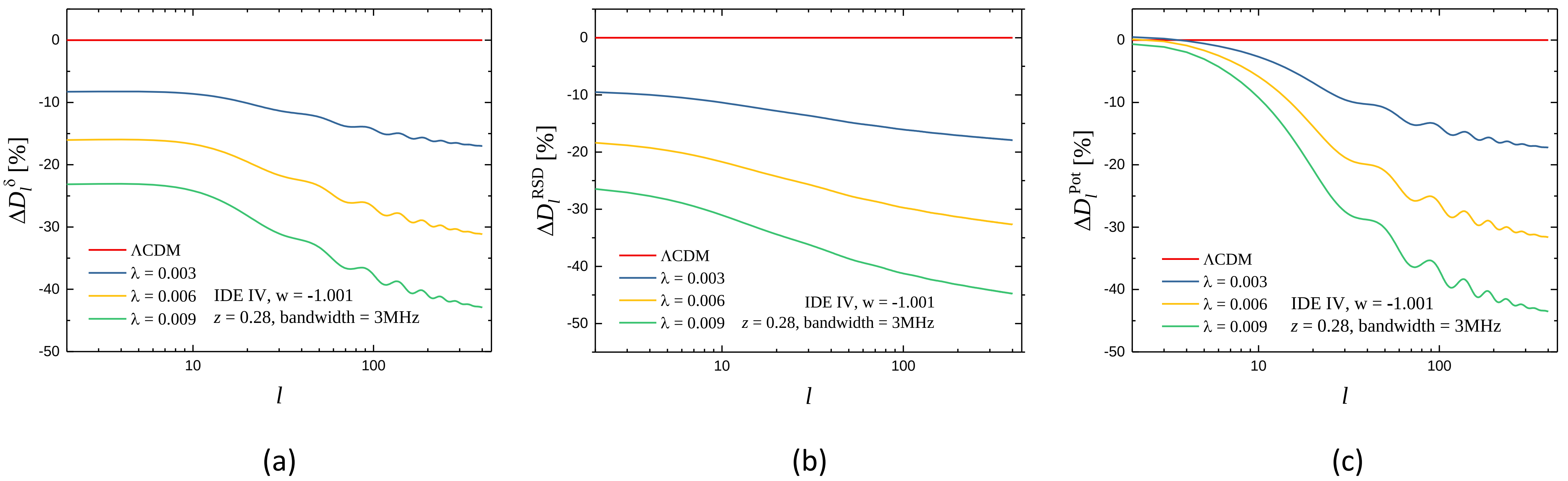

Figure 16 The overdensity, RSD and SW+Potential signals in IDE IV (DE⇒DM) for a varying λ. These weakened signals are closely related to the power suppression showed in Fig. 15.

Some C_l Results

- For *IDE* IV, varying λ:

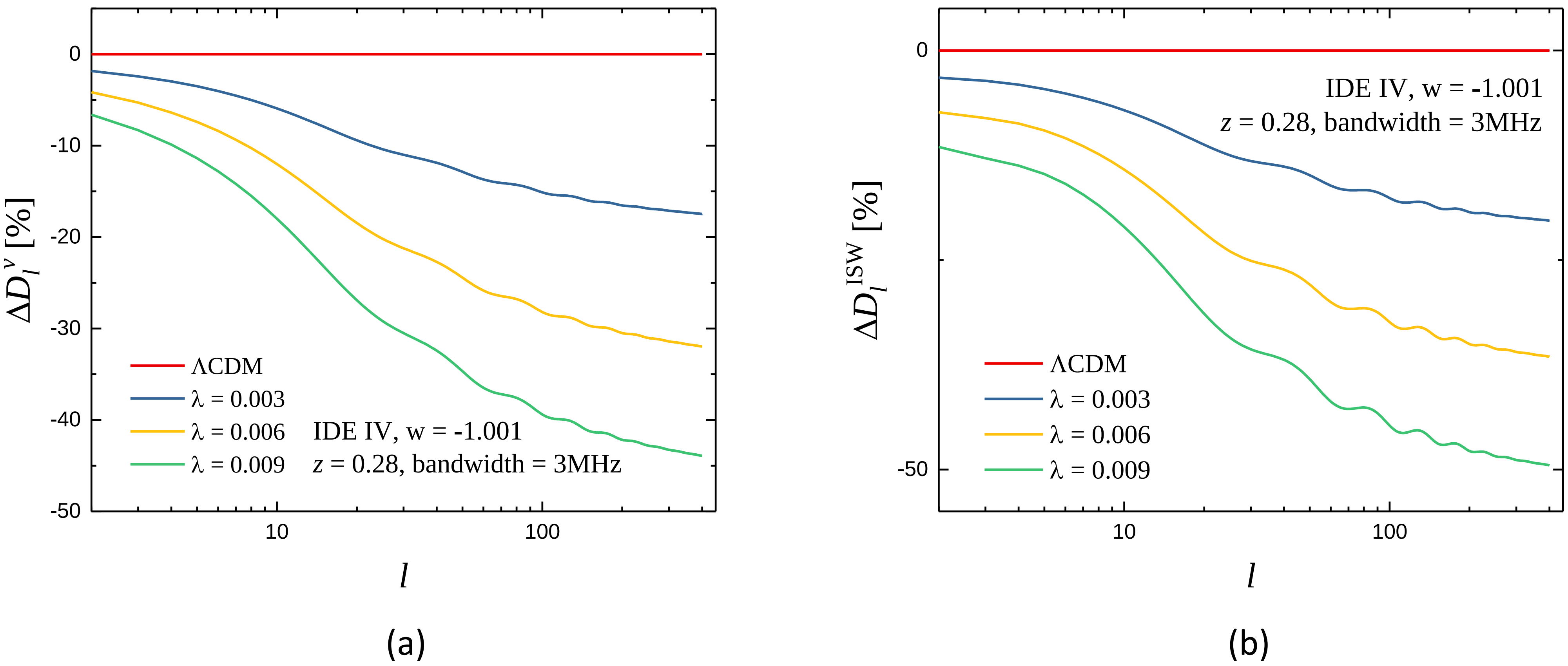

Figure 17 Similar to Fig. 14, but for the Doppler and ISW effects.

Some C_l Results

- For *IDE* IV, varying λ:

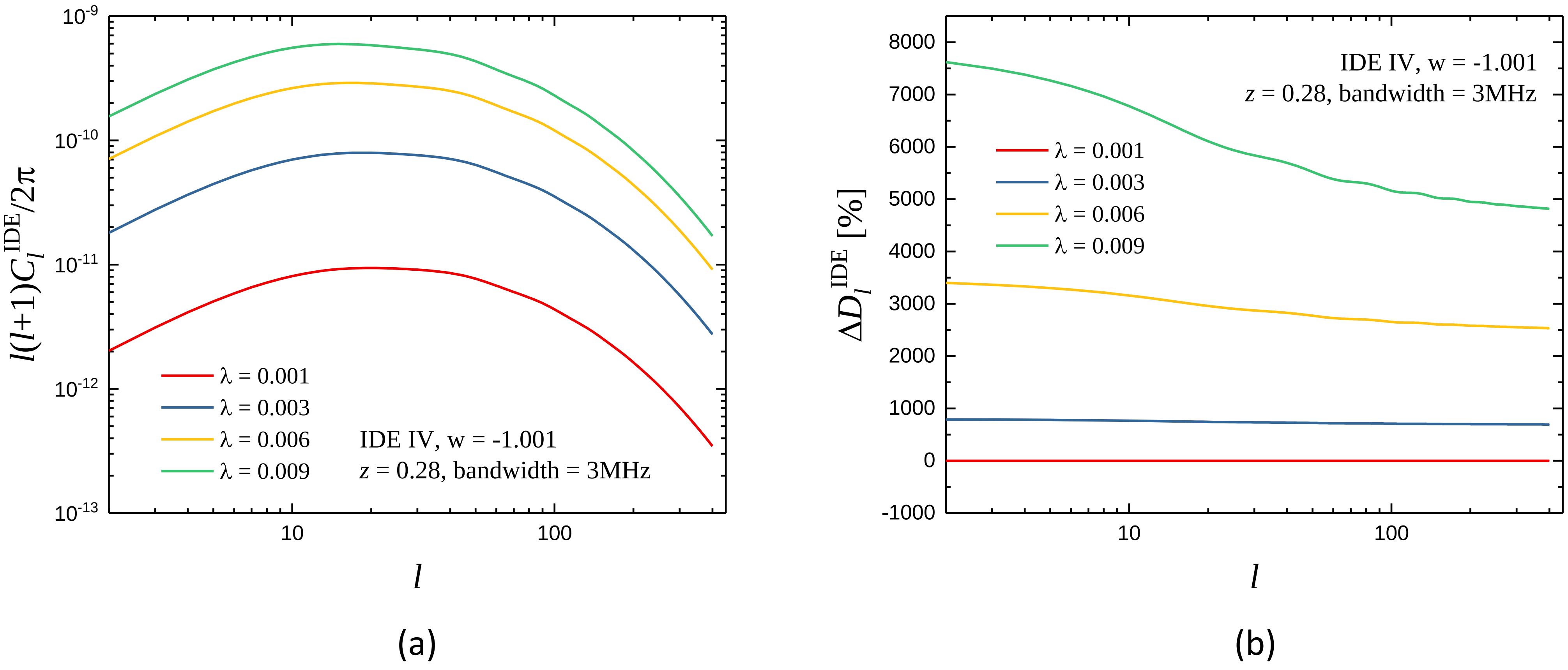

Figure 18 The signal from extra IDE term in IDE IV depends more on the interaction than the equation of state.

Some C_l Results

- For *IDE* I, varying λ_2:

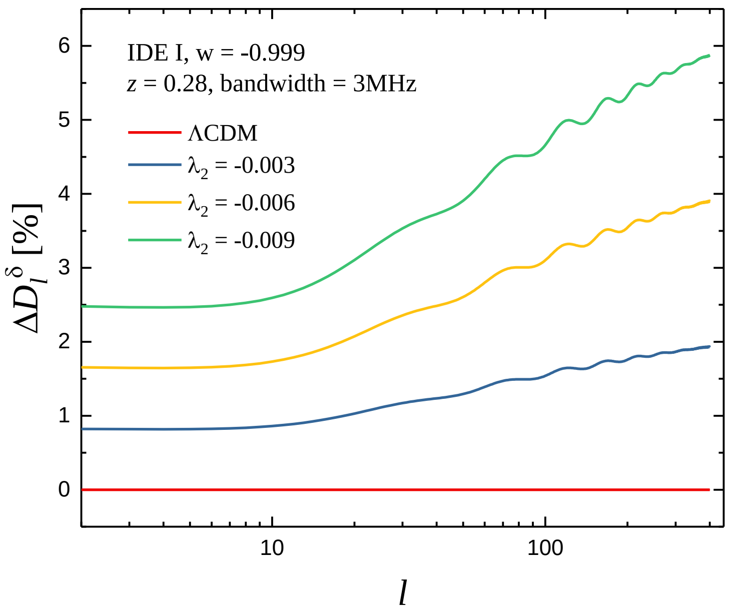

(a)

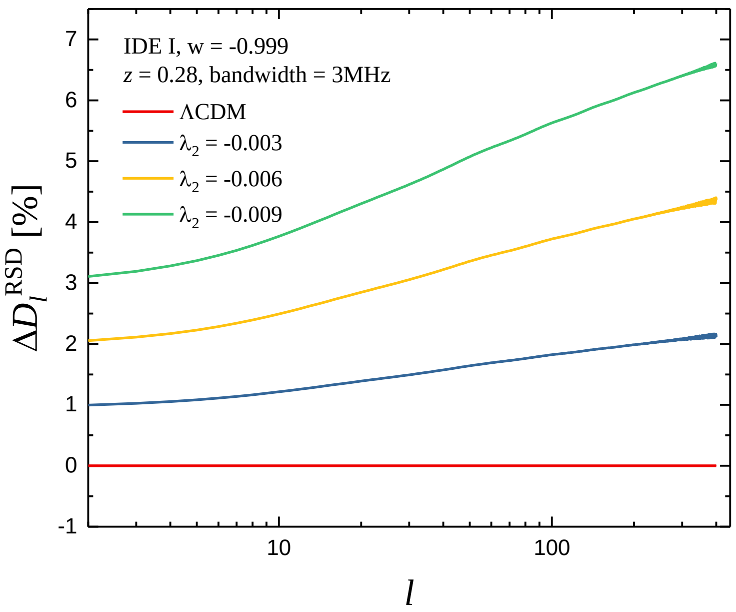

(b)

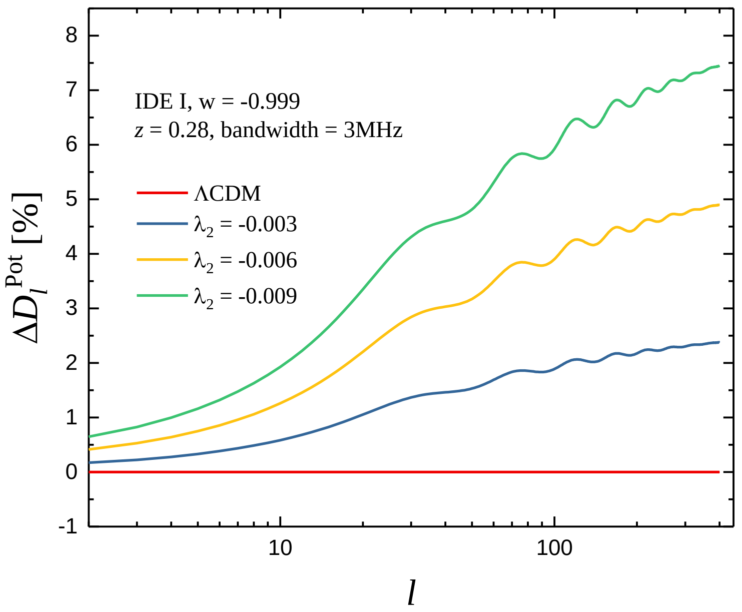

(c)

Figure 19 In contrast to IDE IV, the 21cm signals in IDE I obtain enhancement due to the energy flowing from DM to DE, but the mechanism behind is the same. Also worth noting that, the change to the signals here are much smaller than those in IDE IV.

Some C_l Results

- For *IDE* I, varying λ_2:

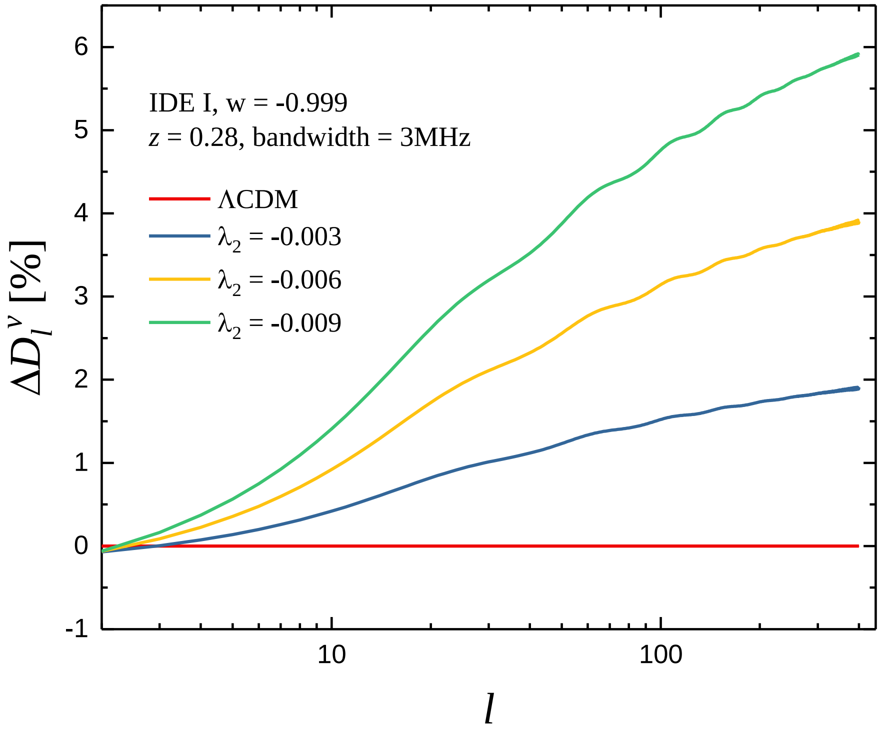

(a)

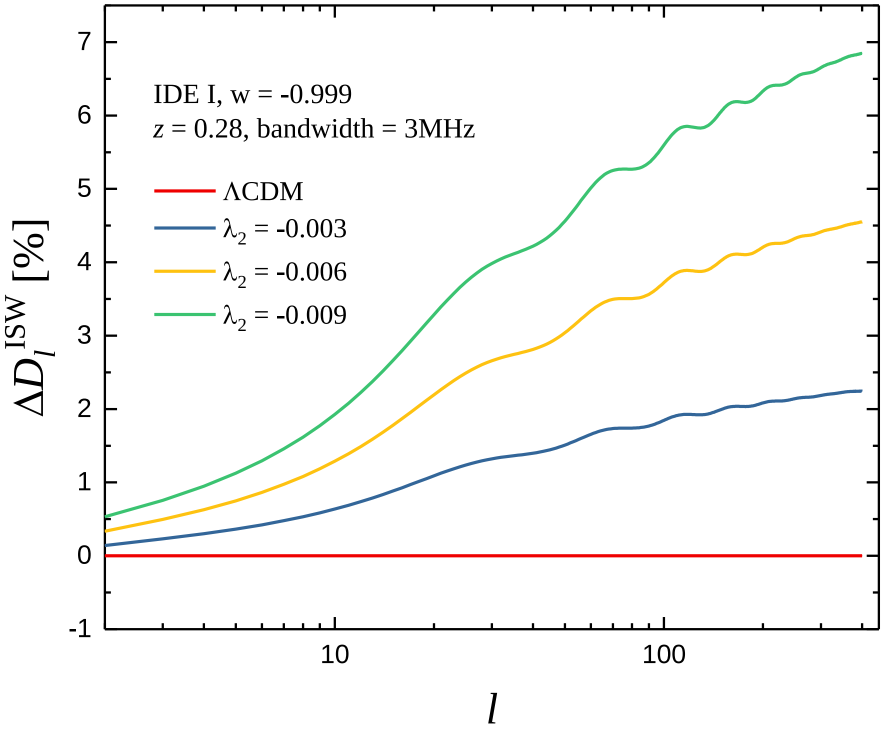

(b)

Figure 20 Similar to Fig. 19, but for the Doppler and ISW effects.

Some C_l Results

- For *IDE* I, varying λ_2:

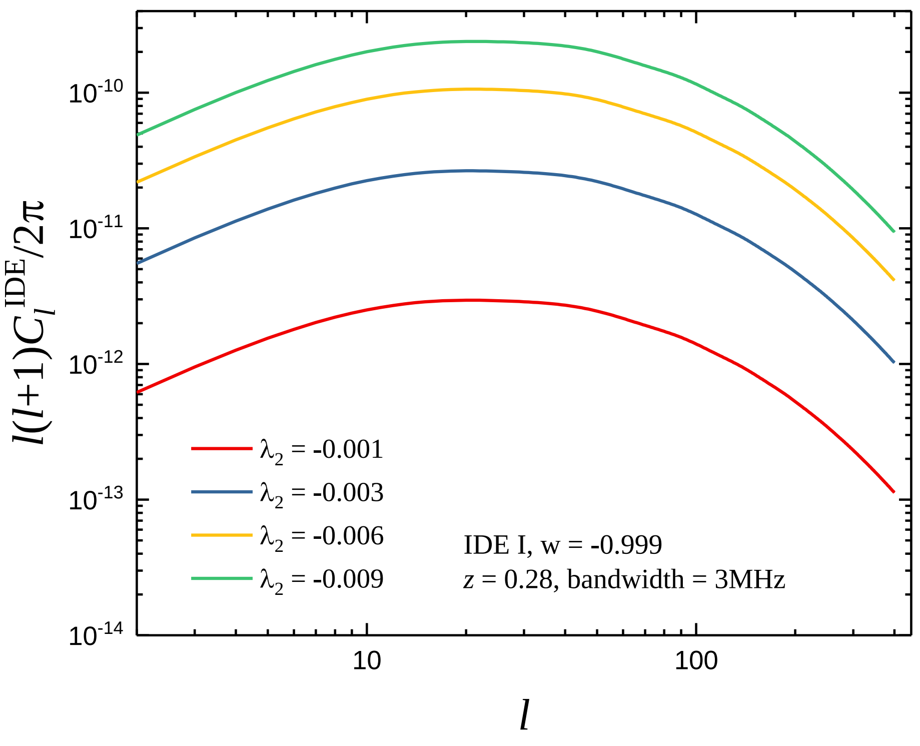

(a)

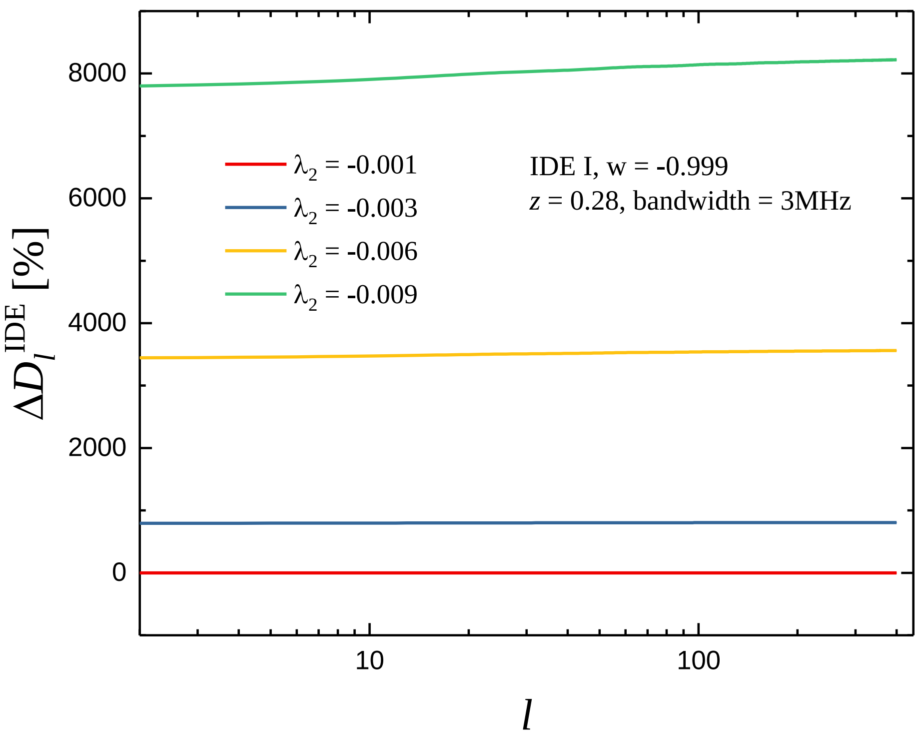

(b)

Figure 21 The magnitude of the extra IDE signal and its discrepancy here are on the same level of those in IDE IV.

Some C_l Results

- For *IDE* I, varying λ_2:

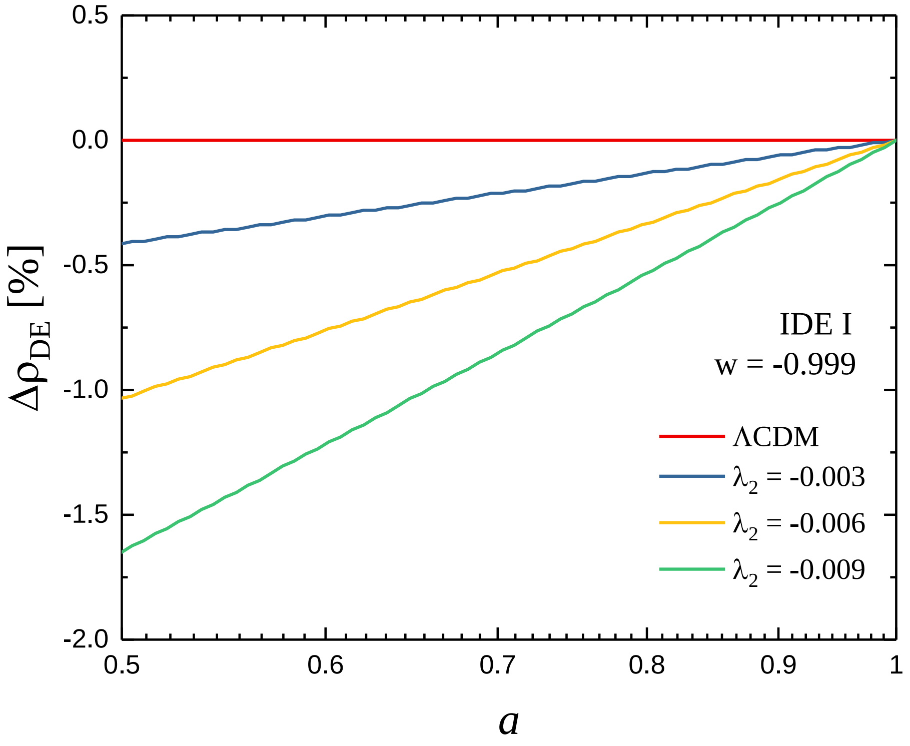

(a)

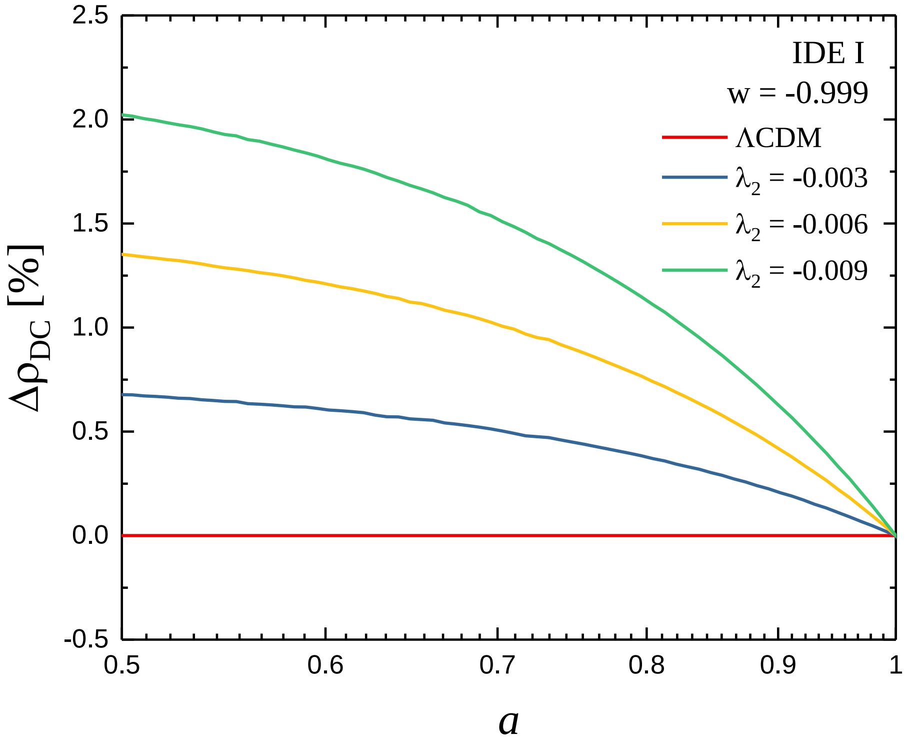

(b)

Figure 22 The background evolution of DE and DM in IDE I (DM⇒DE).

Some C_l Results

- For *IDE I*, varying λ_2:

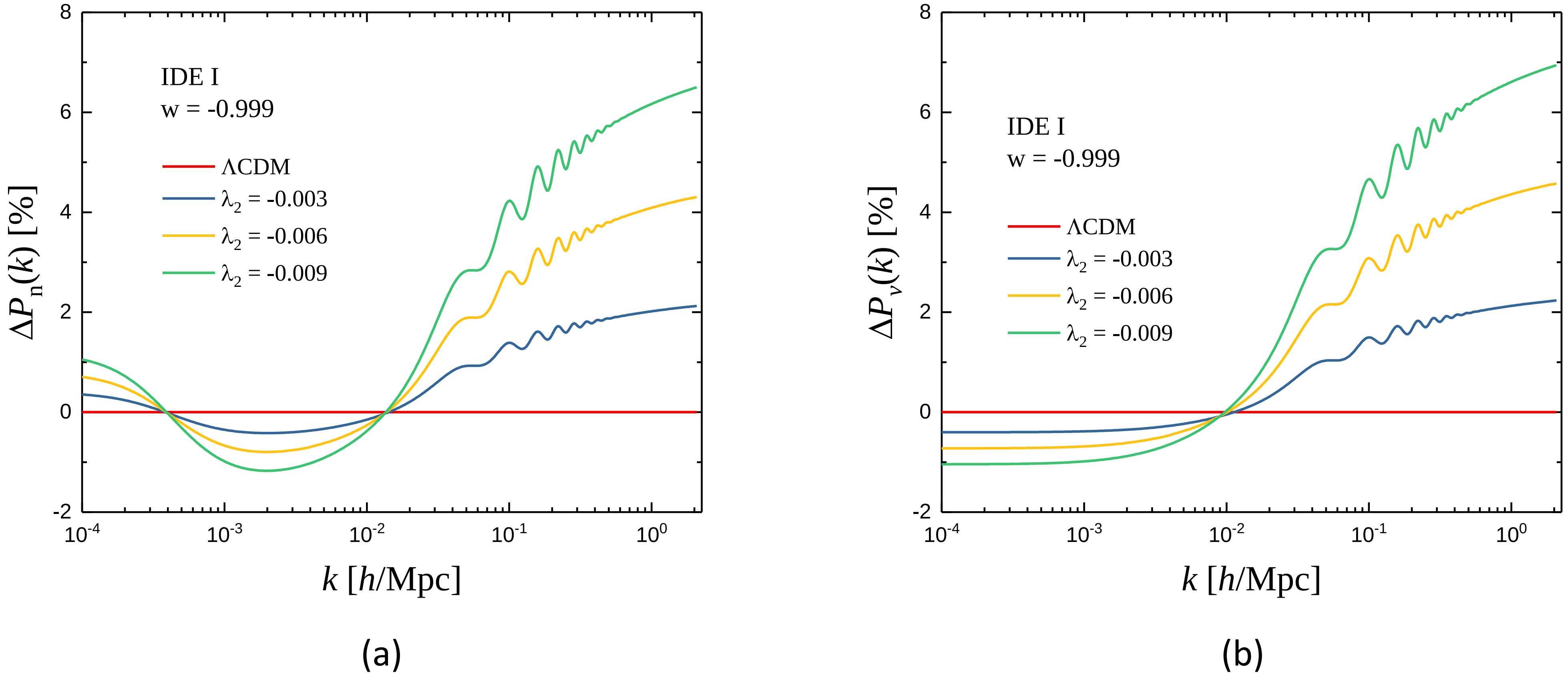

Figure 23 The power discrepancies induced by a varying λ in IDE I (DM⇒DE).

Model & Method

- The *Fisher matrix*:

$$F_{\alpha\beta} = f_{\rm sky} \sum_{\ell_{\rm min}}^{\ell_{\rm max}} \left(\frac{2\ell+1}{2}\right) {\rm Tr}[\Gamma_{\ell,\alpha}(\Gamma_\ell)^{-1}\Gamma_{\ell,\beta}(\Gamma_\ell)^{-1}],$$

f_{sky} is the fractional sky coverage. (f_{sky} = 0.07 for BINGO)

Γ_ℓ is a matrix composed of the cross and autocorrelation angular power spectra between the frequency windows.

$\Gamma_\ell^{ij} = C_\ell^{ij} + \delta^{ij} N_\ell$, where i, j denote the frequency window and N_ℓ is the noise power spectrum.

The off diagonal element of Γ_ℓ are usually much smaller than its diagonal elements.

We assume that the noise between different windows is uncorrelated.

In this study the nonlinear effect is ignored due to the quick increase of noise for ℓ equals a few hundred.

—— *arXiv: 1710.03643*

Fisher Matrix Forecast

- For *IDE I*, comparing *Bingo* & *Bingo+Planck*:

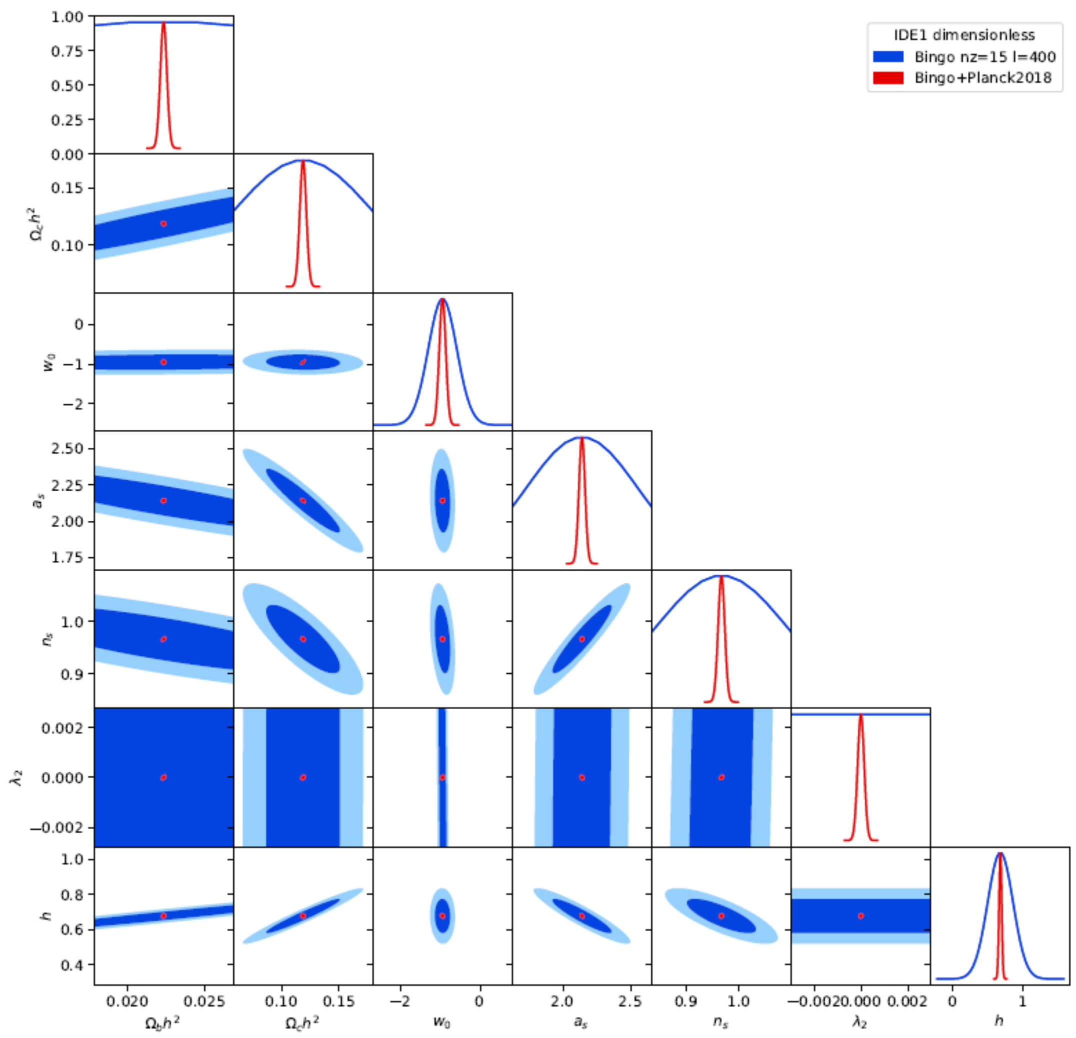

σ	Bingo	Bingo+Planck
$\Omega_c h^2$	0.01409	0.00015
$\Omega_b h^2$	0.04199	0.00199
w_0	0.25255	0.05774
A_s	0.28617	0.01570
N_s	0.08535	0.00437
λ_2	0.03896	0.00010
h	0.12657	0.01290

Fisher Matrix Forecast

- For *IDE* I, with different *bandwidths*:

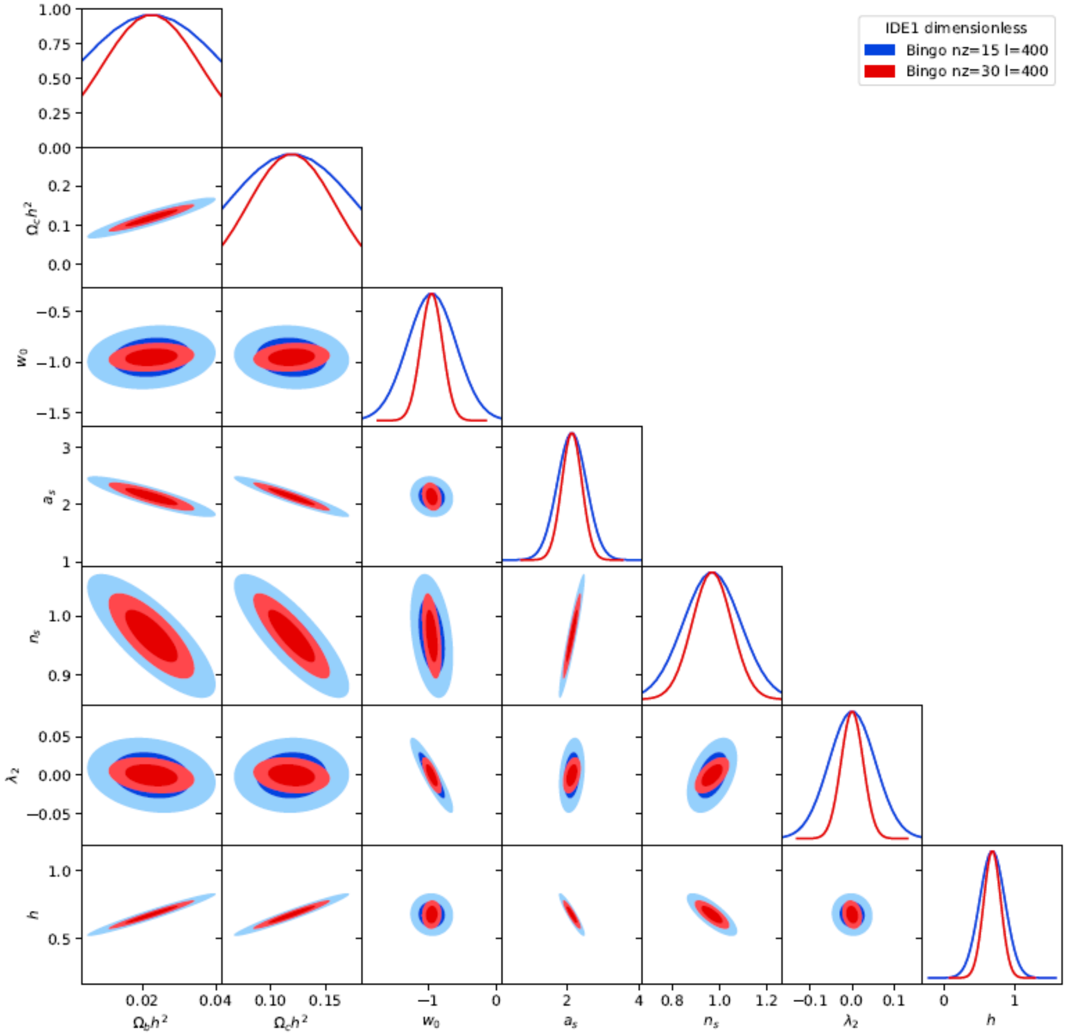

σ	Δv=20MHz	Δv=10MHz
$\Omega_c h^2$	0.01409	0.00941
$\Omega_b h^2$	0.04199	0.02791
w_0	0.25255	0.11261
A_s	0.28617	0.19844
N_s	0.08535	0.05881
λ_2	0.03896	0.01862
h	0.12657	0.08457

Fisher Matrix Forecast

- For *IDE I*, with *RSD* included or not:

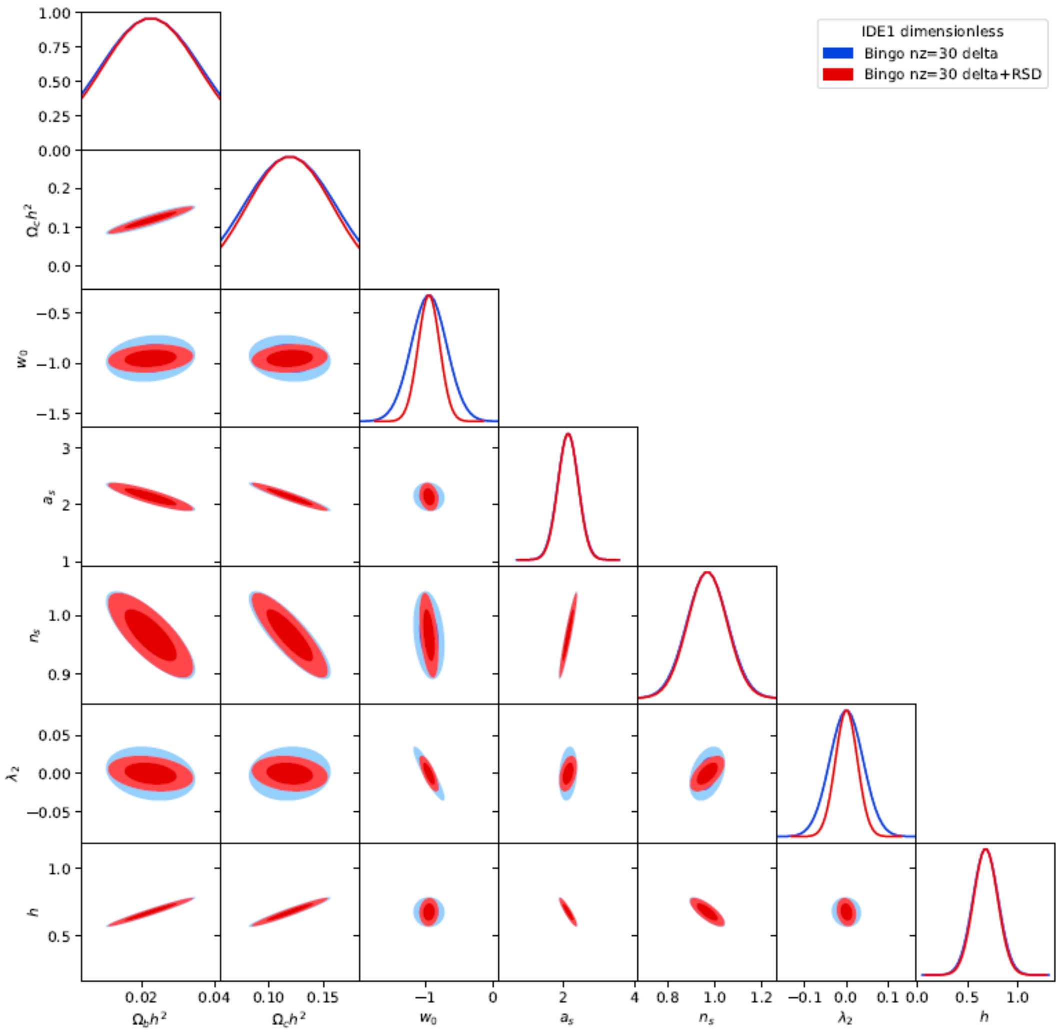

σ	δ	δ+RSD
$\Omega_c h^2$	0.00986	0.00941
$\Omega_b h^2$	0.03007	0.02791
w_0	0.18515	0.11261
A_s	0.20380	0.19844
N_s	0.06102	0.05881
λ_2	0.02825	0.01862
h	0.08889	0.08457

Fisher Matrix Forecast

- For *IDE I*, comparing with *1710.03643* :

σ	Δν=20MHz
$\Omega_c h^2$	0.01409
$\Omega_b h^2$	0.04199
w_0	0.25255
A_s	0.28617
N_s	0.08535
λ_2	0.03896
h	0.12657

Fisher Matrix

	BINGO
σ_w	4.03×10^{-2}
σ_{ξ_1}	N/A
σ_{ξ_2}	1.60×10^{-2}

MCMC *Planck* Only

	Model I ($w > -1,\ \xi_1 = 0,\ \xi_2 < 0$)
w	$-9.031^{+0.23}_{-0.959} \times 10^{-1}$
ξ_1	N/A
ξ_2	$-1.297^{+1.30}_{-0.448} \times 10^{-1}$

Fisher Matrix Forecast

- For ΛCDM, comparing with *1707.07647* :

σ	Baseline	Bingo+Planck
$\Omega_c h^2$	0.02218	0.00013
$\Omega_b h^2$	0.1205	0.00118
w_0	-1.0	0.06323
A_s	2.1955e-9	0.02781
N_s	0.9616	0.00414
h	0.668	0.01651

Parameters	Baseline	*Planck* + BINGO (baseline)
$\Omega_b h^2$	0.02224	0.02218 ± 0.00014
$\Omega_c h^2$	0.1198	0.1205 ± 0.0014
h	0.673	0.668 ± 0.009
τ	0.081	0.077 ± 0.017
n_s	0.9641	0.9616 ± 0.0047
$\ln(10^{10} A_s)$	3.096	3.089 ± 0.033
w	-1.0	-1.00 ± 0.04
$\Omega_{\rm HI}\ (\times 10^4)$	6.20	6.33 ± 0.22

Fisher Matrix Forecast

- For *IDE* IV, comparing *Bingo* & *Bingo+Planck*:

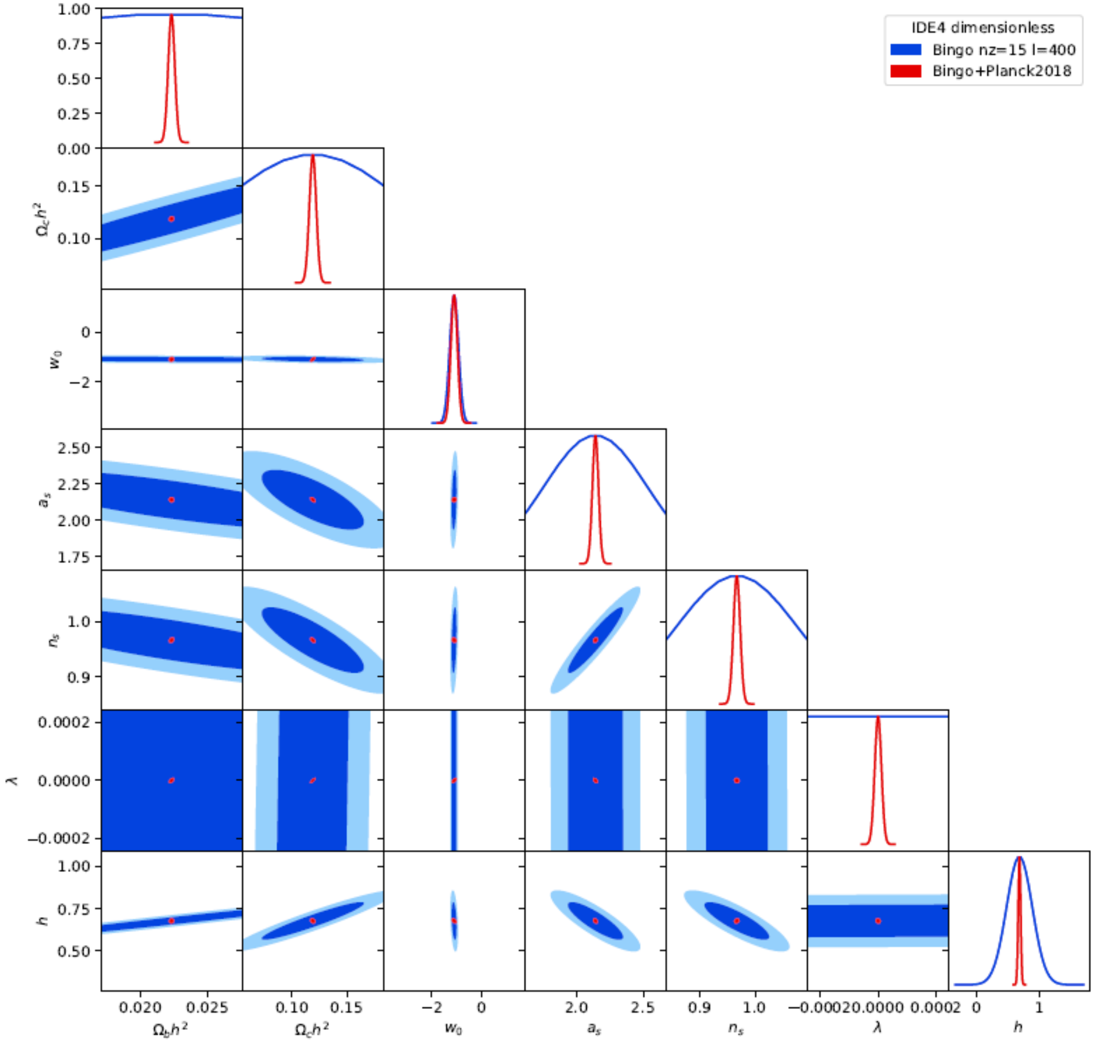

σ	Bingo	Bingo+Planck
$\Omega_c h^2$	0.01670	0.00017
$\Omega_b h^2$	0.06056	0.00219
w_0	0.12371	0.09299
A_s	0.27035	0.01600
N_s	0.07771	0.00436
λ	0.01036	0.000008
h	0.14507	0.01364

Fisher Matrix Forecast

- For *IDE* IV, with different *bandwidths*:

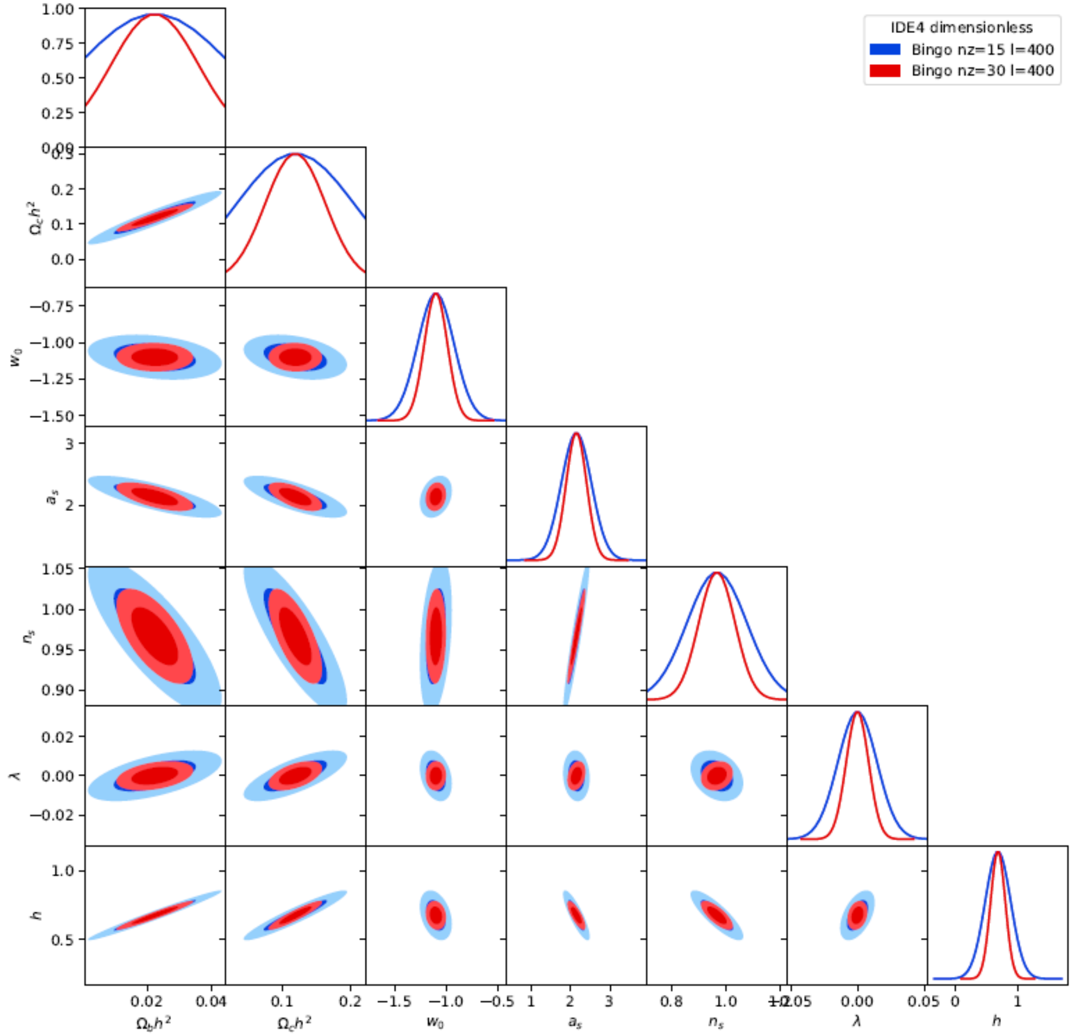

σ	Δv=20MHz	Δv=10MHz
$\Omega_c h^2$	0.01670	0.00954
$\Omega_b h^2$	0.06056	0.03115
w_0	0.12371	0.07851
A_s	0.27035	0.18395
N_s	0.07771	0.04700
λ	0.01036	0.00594
h	0.14507	0.08340

Fisher Matrix Forecast

- For *IDE* IV, with *RSD* included or not:

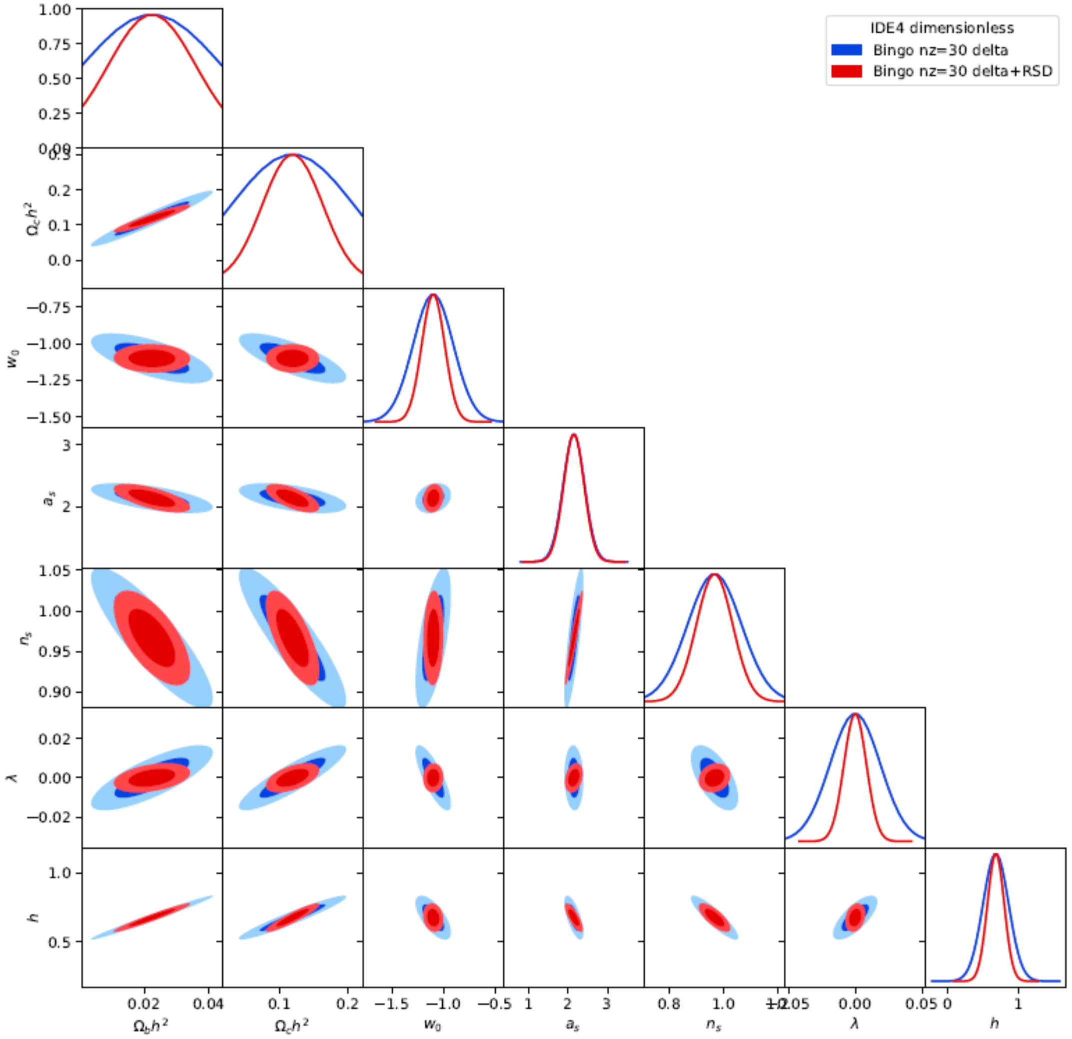

σ	δ	δ+RSD
$\Omega_c h^2$	0.01519	0.00954
$\Omega_b h^2$	0.06287	0.03115
w_0	0.13717	0.07851
A_s	0.19302	0.18395
N_s	0.06981	0.04700
λ	0.01327	0.00594
h	0.12753	0.08340

Conclusions & Prospections

- *Density fluctuation* and *RSD* are the two leading components of the total 21cm C_ls.
- In addition to an extra term, $v_m \frac{a^2 Q_c^0}{\rho_m}$, the interaction will leave some marks on every component of the brightness temperature fluctuation.
- The equation of state w plays a similar role in the *IDE* scenario as it does in ΛCDM, and thus the effects from the *interaction* is easily identified, especially those on small scales.
- *More* DM and/or *less* DE during the cosmic expansion prefer to *enhance* every component of the 21cm signals, except for the extra IDE contribution which is proportional to the strength of the interaction.
- The power of *BINGO* alone on parameter constraints is much weaker than that of *Planck*.
- Including *RSD* or narrowing the *bandwidth* is beneficial for a tighter constraint.

Some C_l Results

- For ΛCDM :

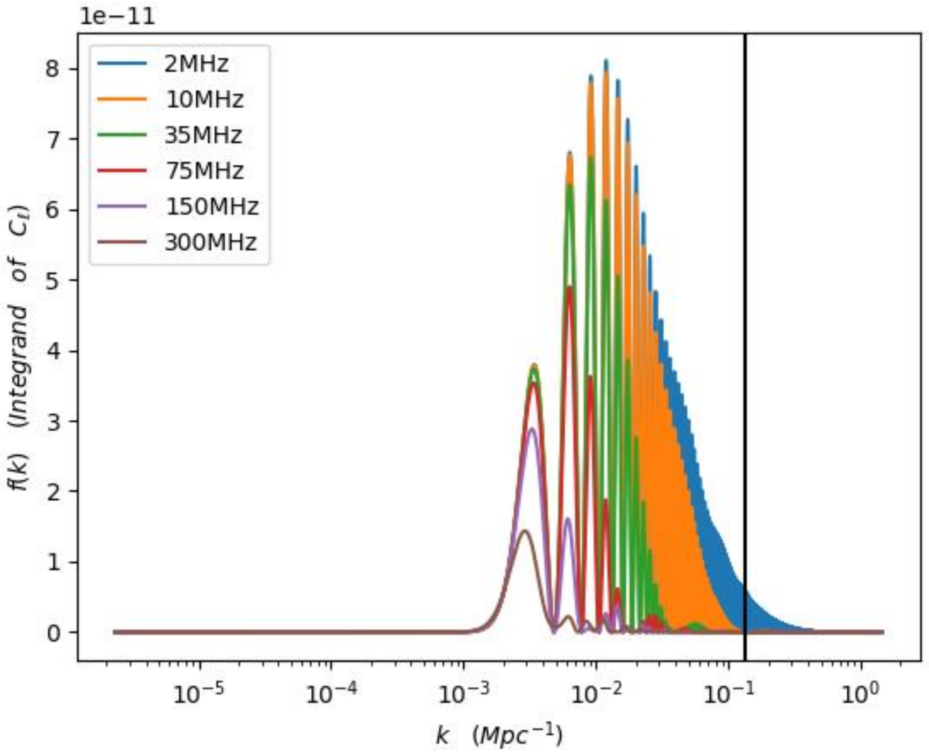

$l = 2$

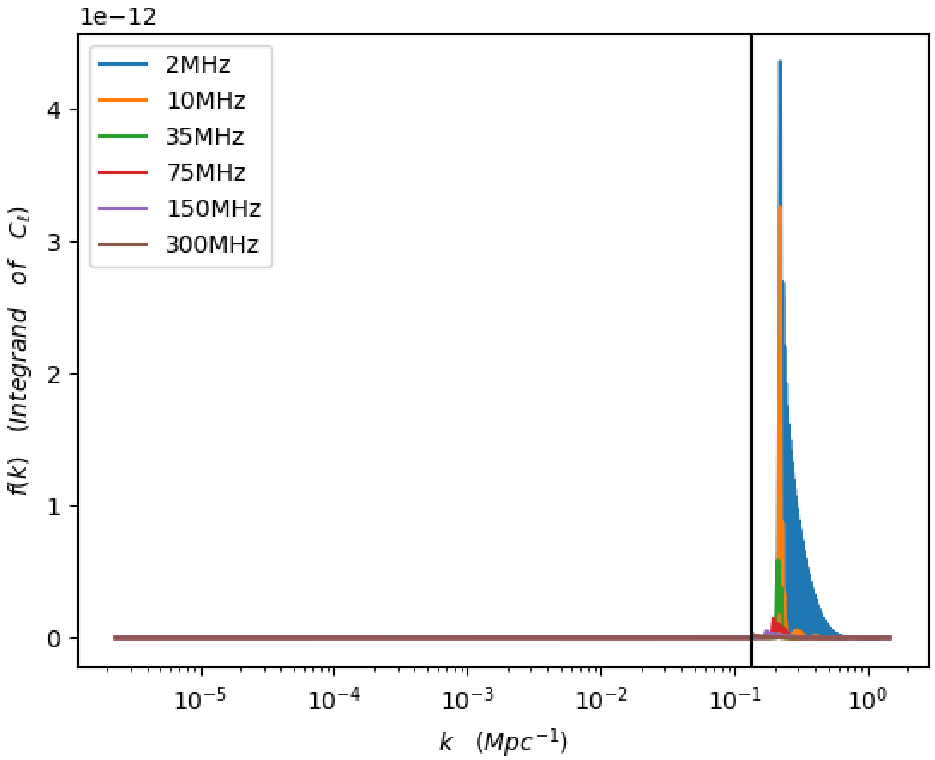

$l = 250$

Some C_l Results

- For ΛCDM :

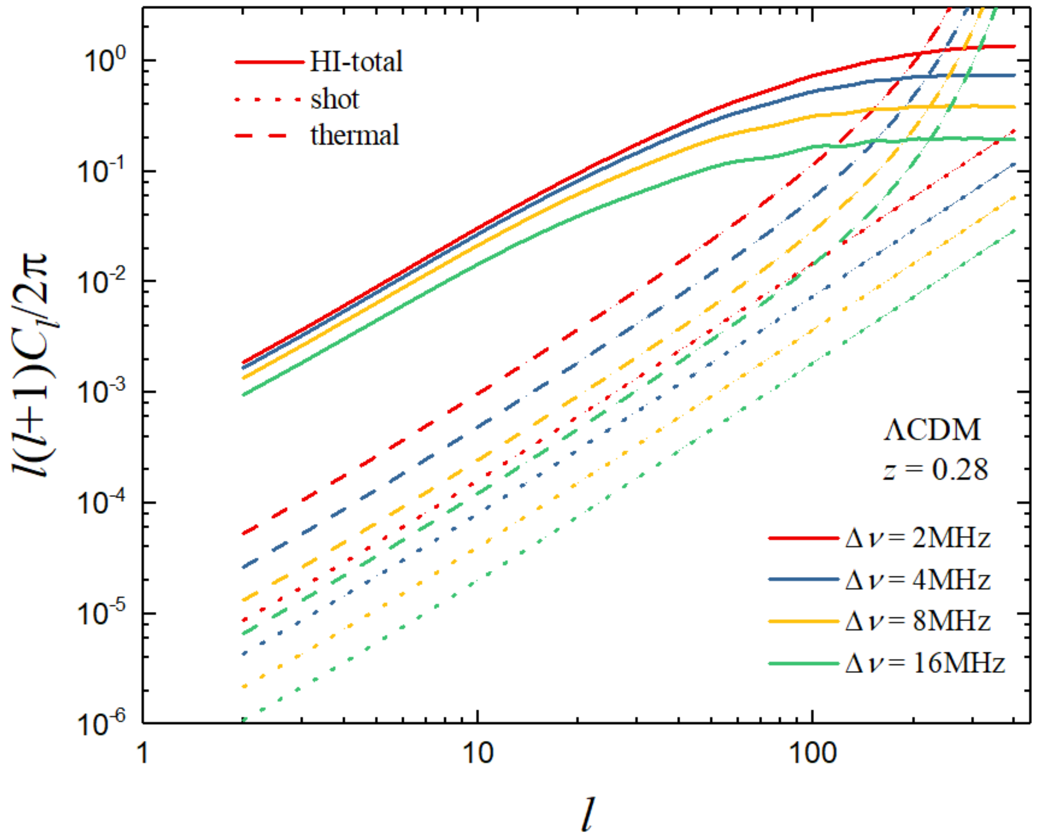

- The effects of the bandwidth
- Necessary to consider the nonlinearity?
- How RSD affects through the bandwidth?

Some C_l Results

- For ΛCDM :

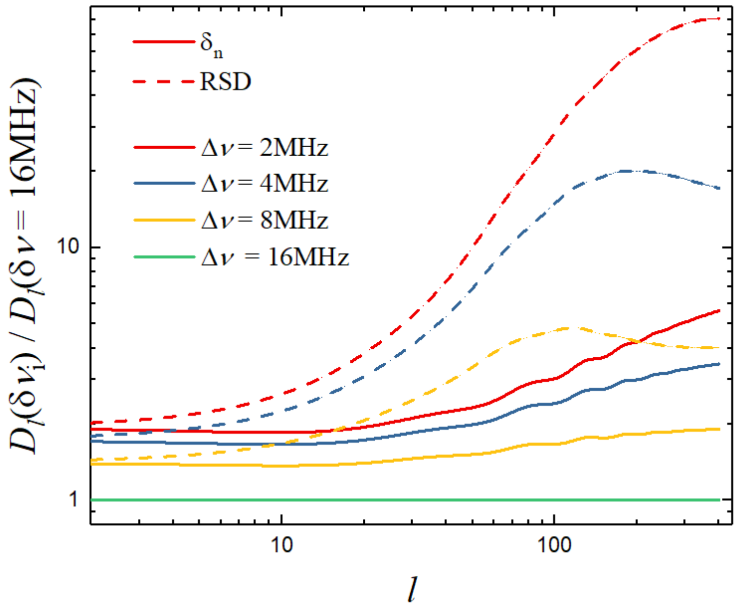

(a)

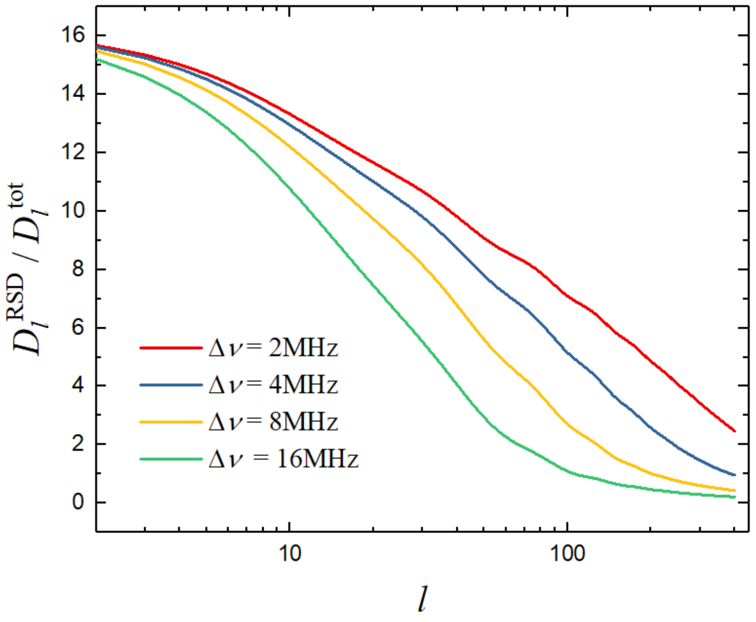

(b)

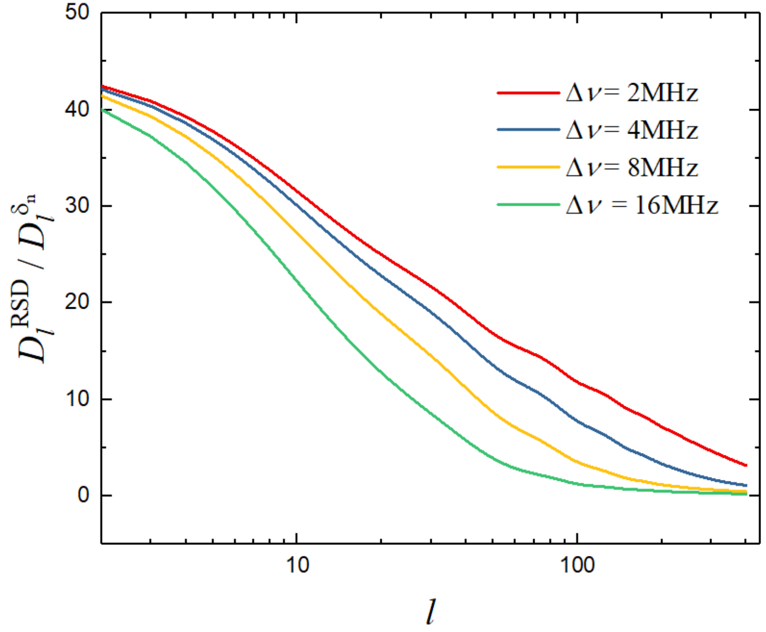

(c)

Some C_l Results

- For *IDE* I :

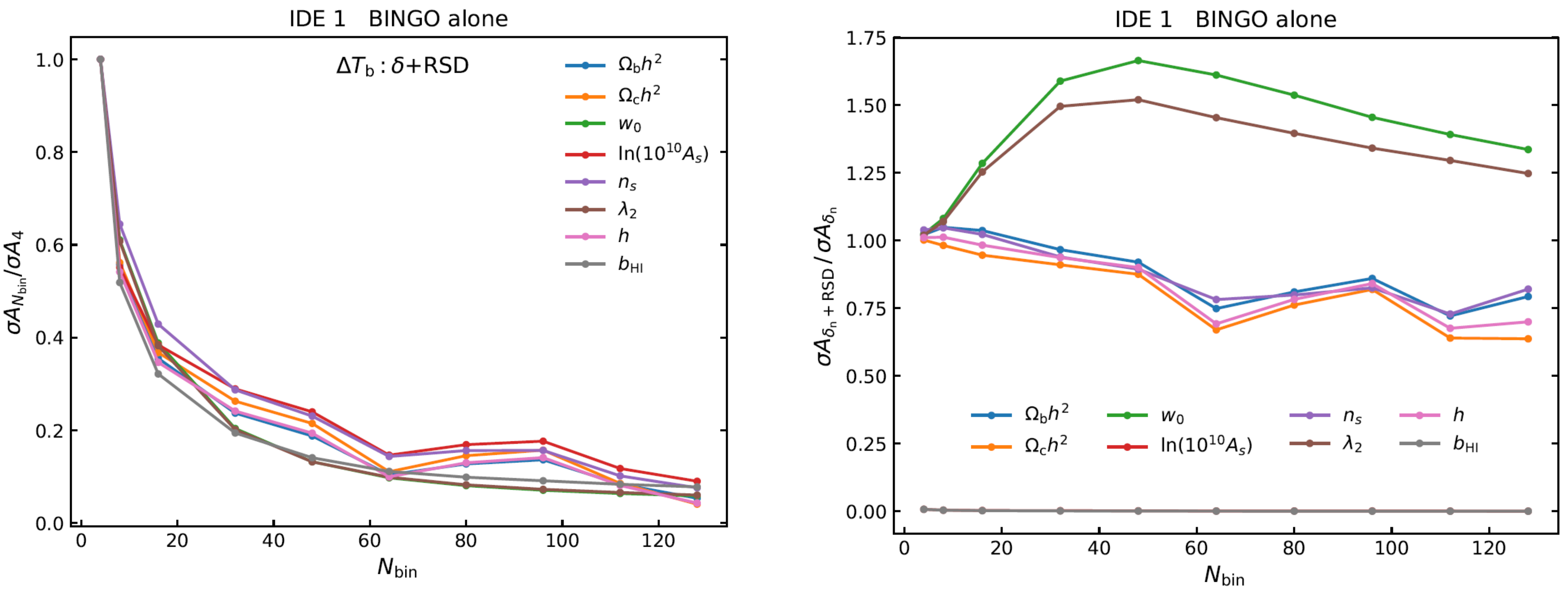

Some C_l Results

- For *IDE* I :

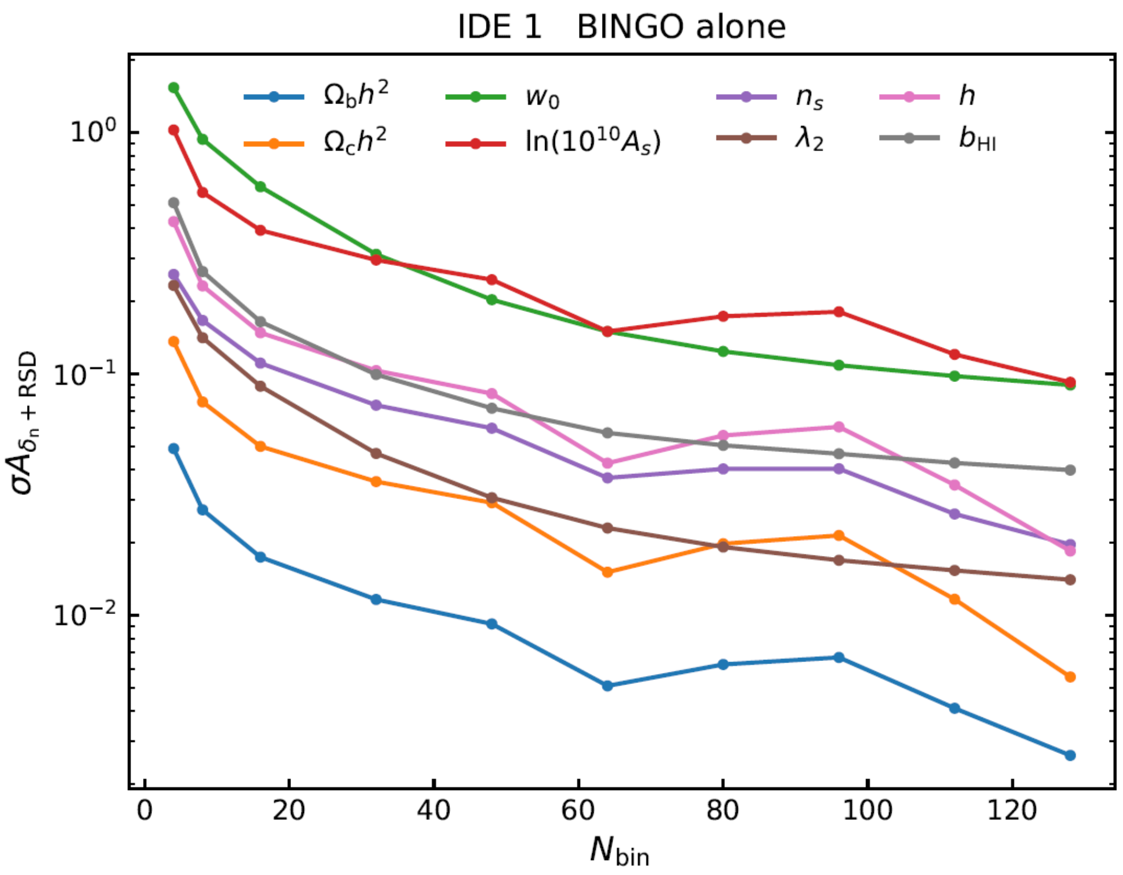

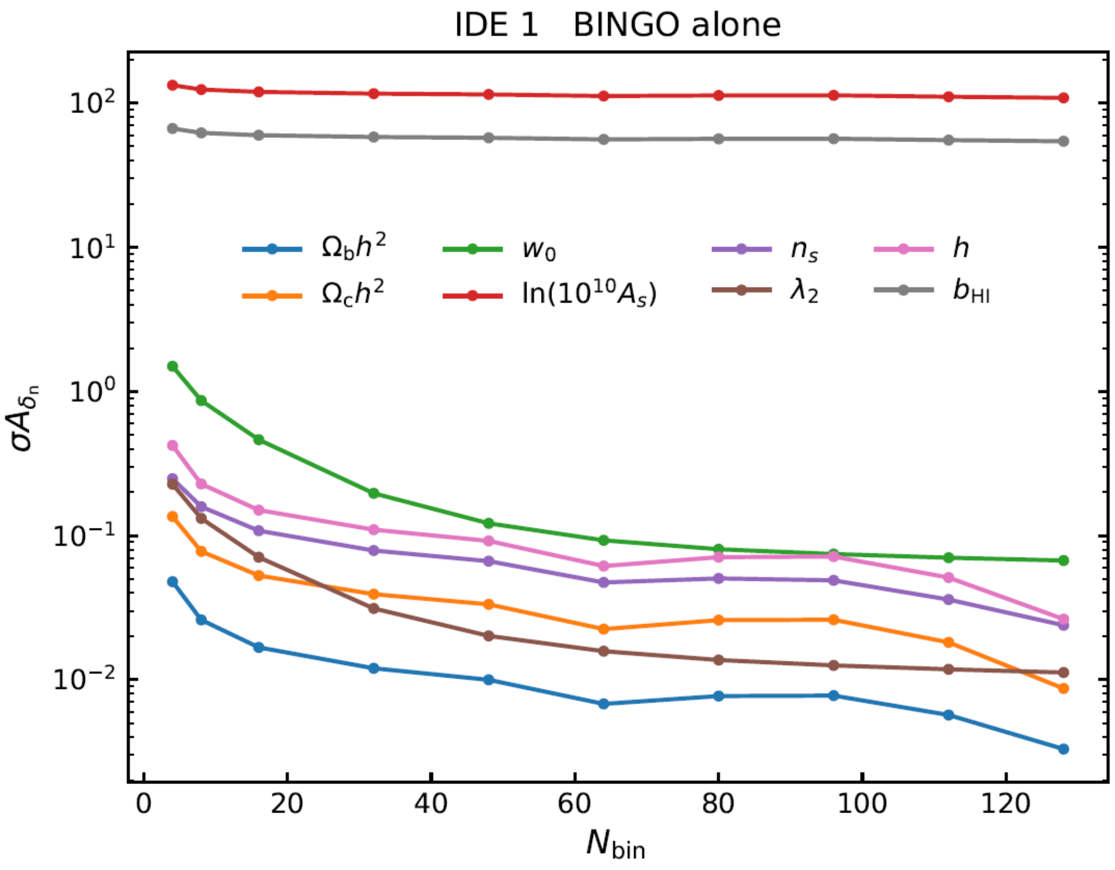

Some C_l Results

- For *IDE* I :

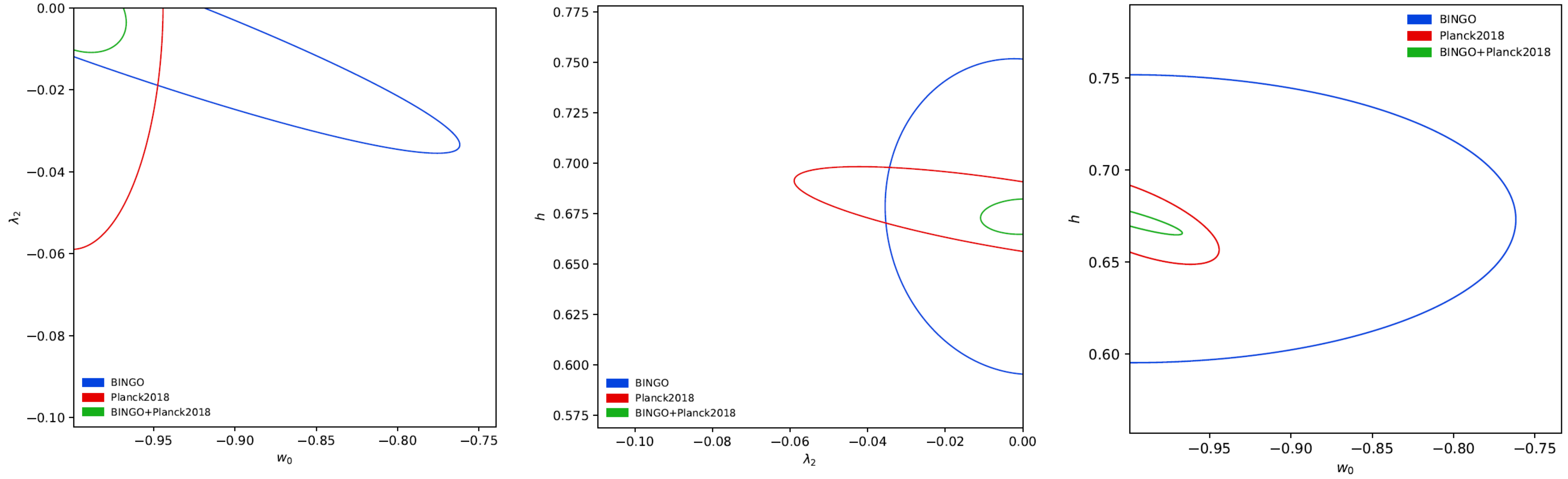

(a) (b) (c)

Some C_l Results

- For $\mathcal{IDE}$ I :

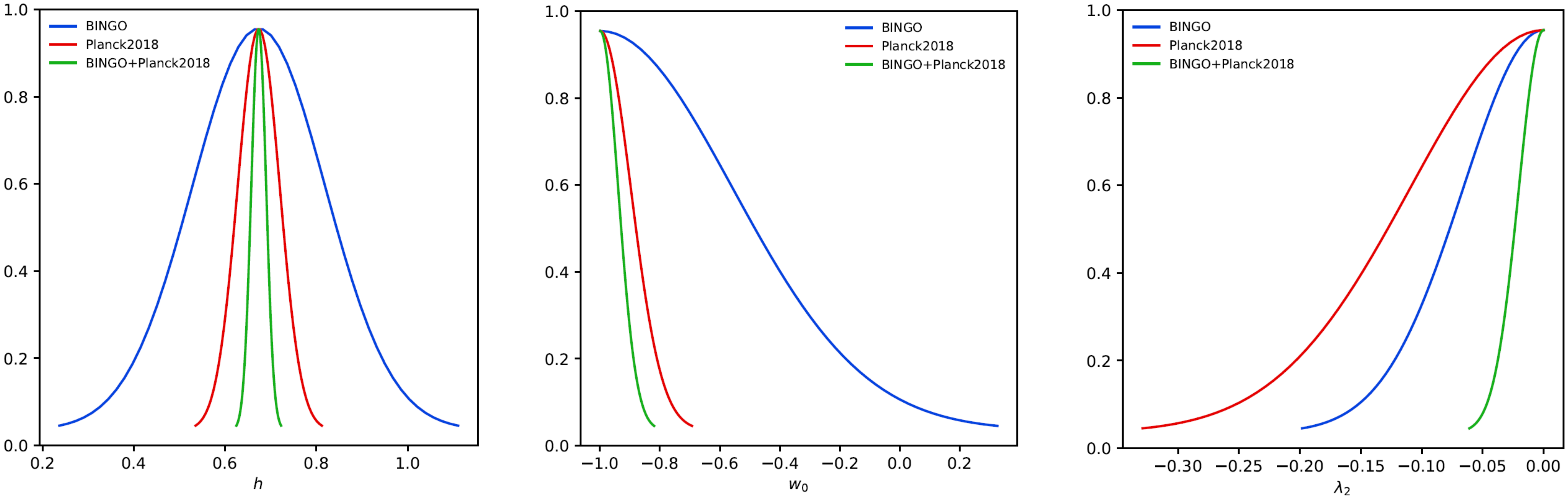

(a) (b) (c)

Some C_l Results

- For *IDE* IV :

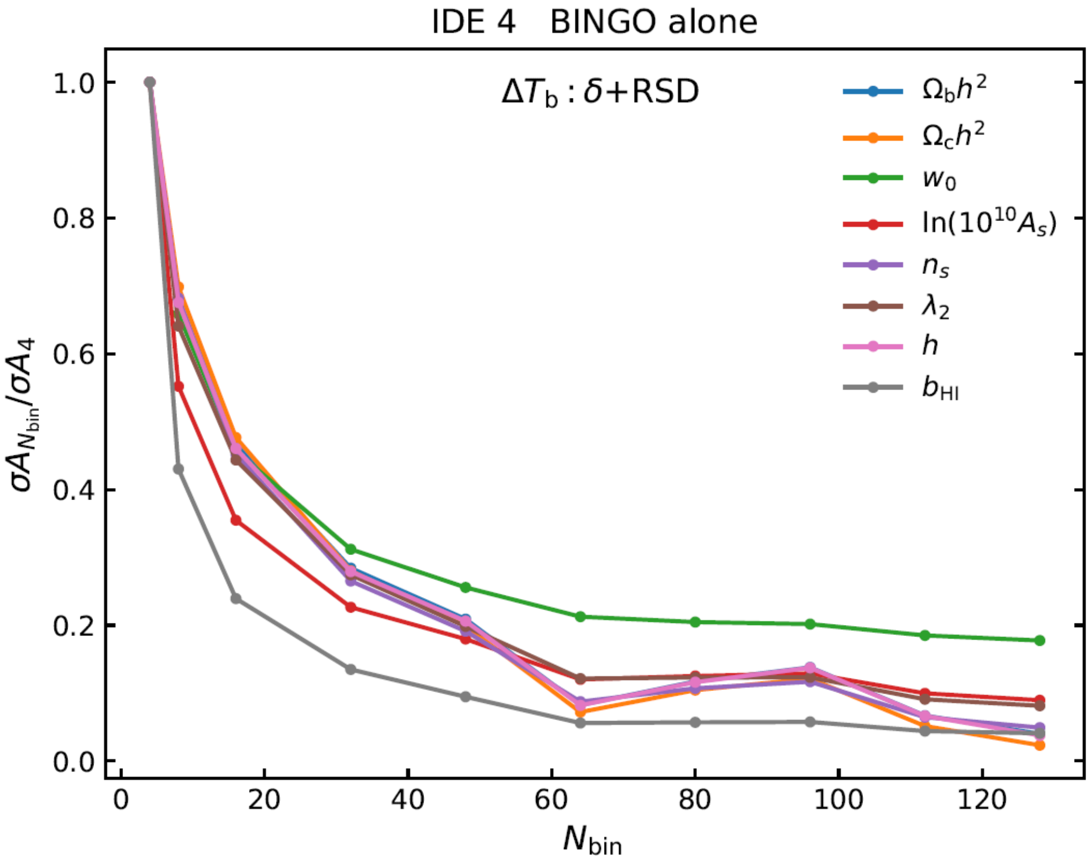

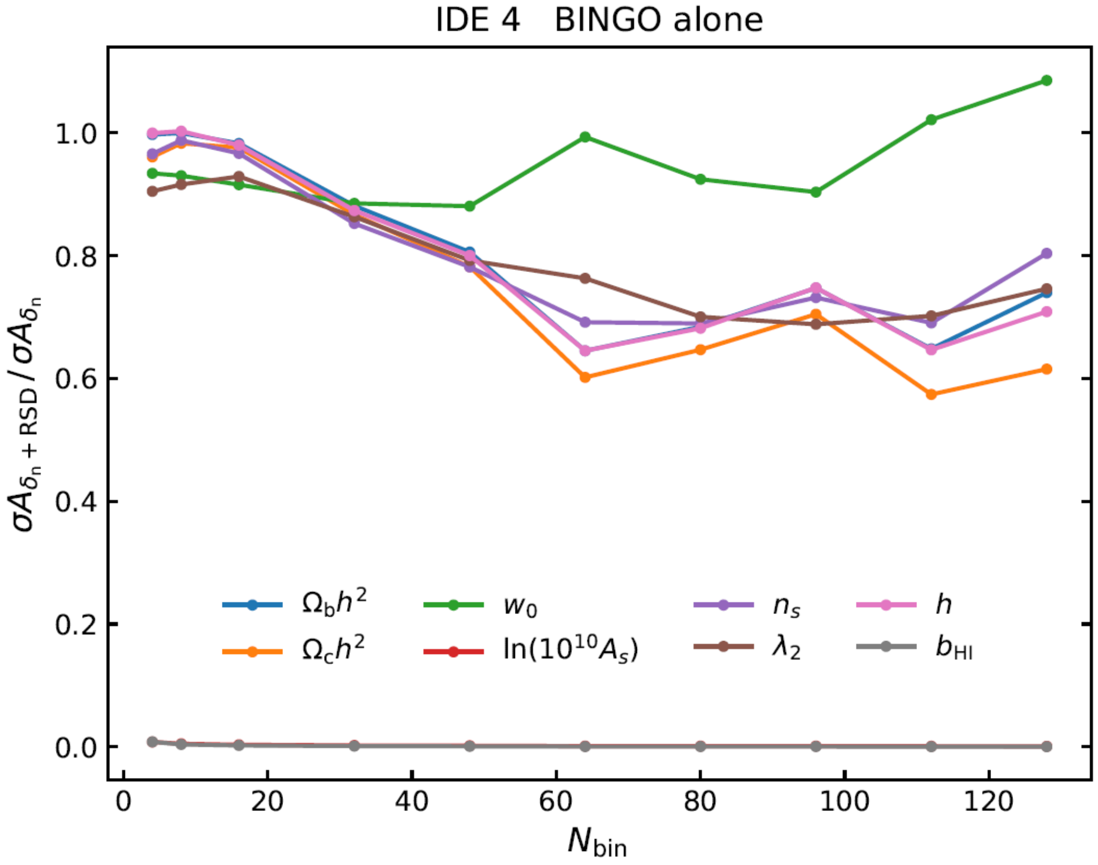

Some C_l Results

- For $\mathcal{IDE}$ IV :

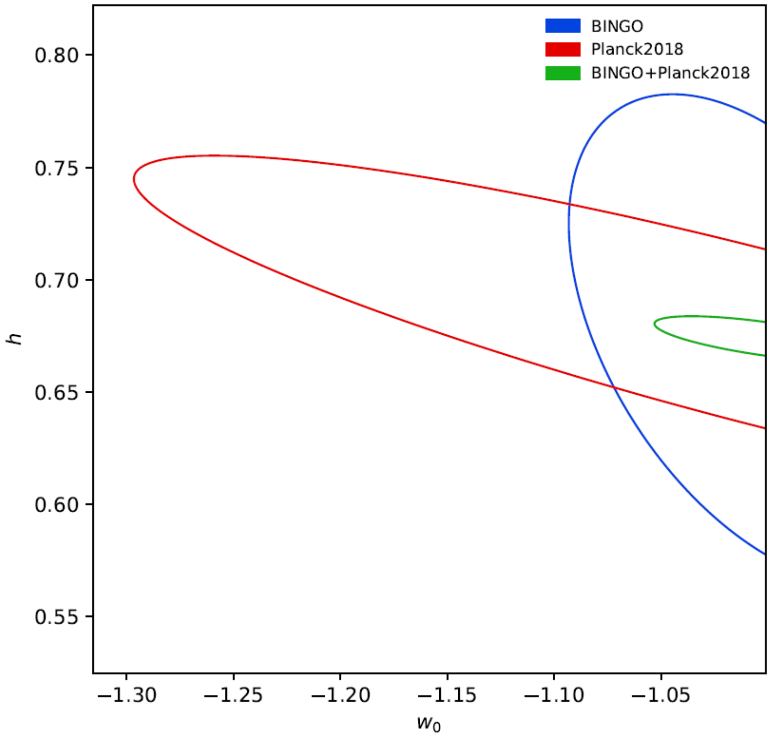

(a)

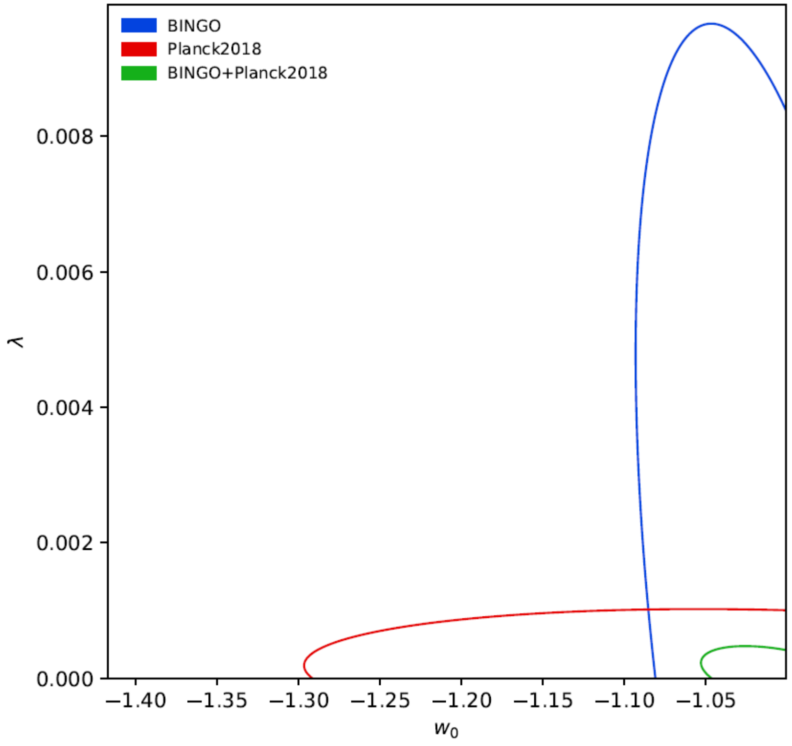

(b)

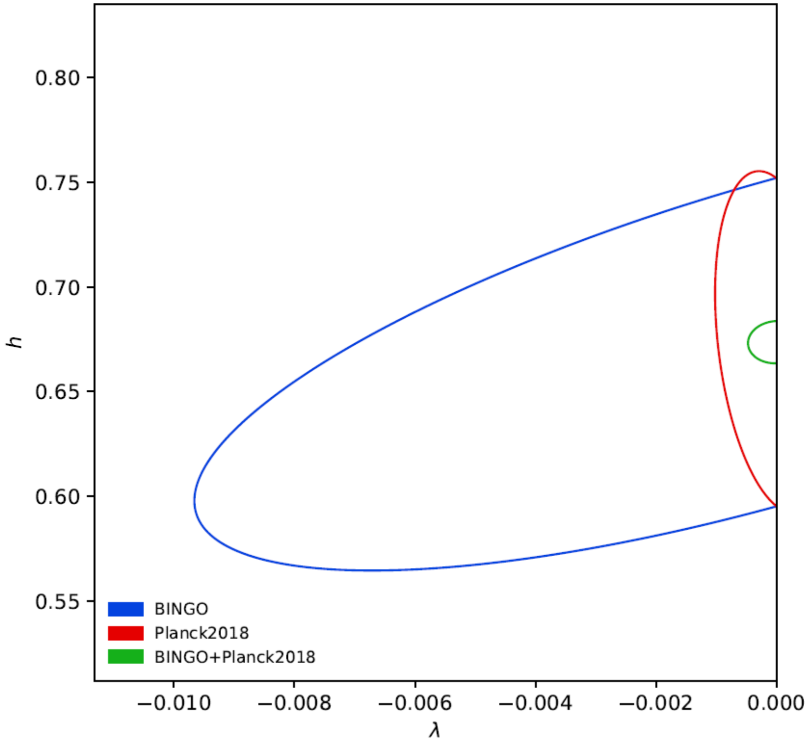

(c)

Some C_l Results

- For $\mathcal{IDE}$ IV :

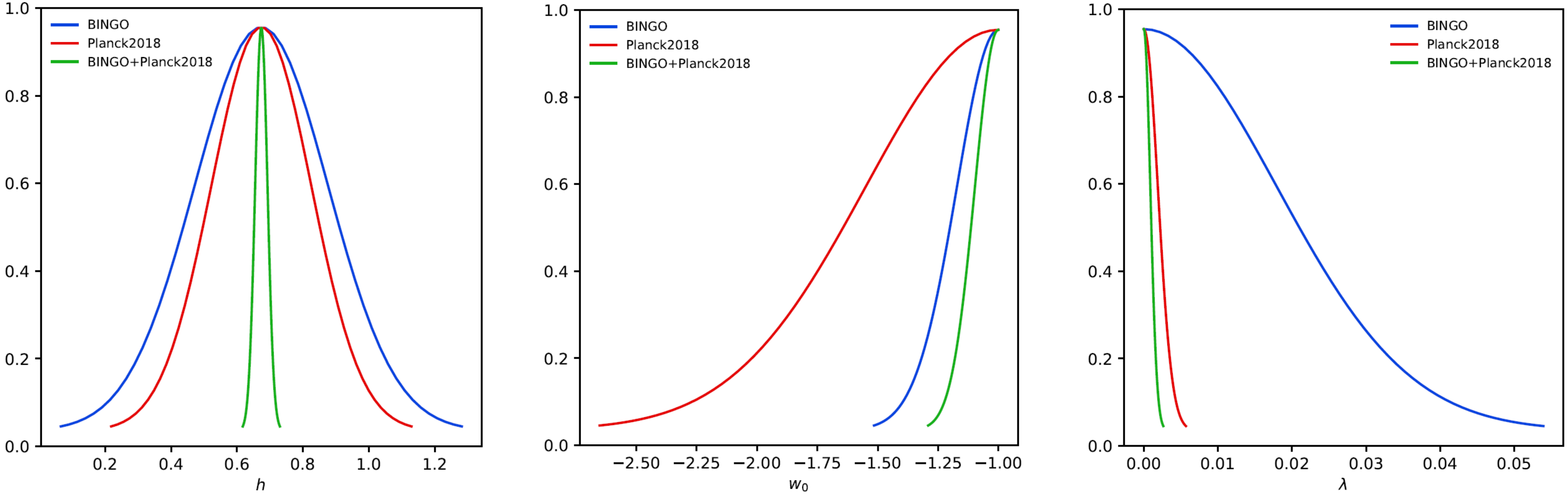

(a) (b) (c)


Thank You